1-1-2013

Study of Porous, Crystalline Supramolecular Boronates

Vincenzo Michael DiSantis
University of South Carolina - Columbia

STUDY OF POROUS, CRYSTALLINE SUPRAMOLECULAR BORONATES

by

Vincenzo Michael DiSantis

Bachelor of Science
Saint Vincent College, 2011

Submitted in Partial Fulfillment of the Requirements

For the Degree of Master of Science in

Chemistry

College of Arts and Sciences

University of South Carolina

2013

Accepted by:

John Lavigne, Director of Thesis

Daniel Reger, Reader

Lacy Ford, Vice Provost and Dean of Graduate Studies

Dedication

This work is dedicated my family, especially my father Michael J. DiSantis and my mother Gabriella DiSantis for their love, support and guidance that has given me the opportunity to pursue my goals in life.

Acknowledgements

I would to thank my family for all the support and encouragement they have given me over the years. I would especially like to thank my parents for their guidance and for always pushing me to achieve excellence in everything that I pursue. If it were not for my parents, I would not be where I am today. Next, I would like to thank all of my friends who have allowed me have a great experience during my time in South Carolina. I would also like to thank Stella whose happiness and joy has always been able to put a smile on my face. A big thank you to all of my lab-mates in the Lavigne group, past and present that helped me along the way. I would like to thank Dr. Robert Green for his help with PXRD and Dr. Mark Smith for his help in crystallography.

I would like to thank my committee members Dr. Daniel Reger, Dr. Linda. Shimizu, and Dr. Nicole Berge for their advice and words of wisdom. A special thank you to my advisor Dr. John Lavigne for mentoring me and giving advice on my research. Finally, I would like to thank the Department of Chemistry and Biochemistry at the University of South Carolina for their support and the opportunity to earn my Master's Degree in Chemistry.

Abstract

Porous materials with the ability to selectively absorb volatile organic compounds are of high interest for applications in sensing, sequestration and separations. Utilizing the covalent yet reversible boronate ester bonds between boronic acids and diols in conjunction with dative boron-nitrogen coordination bonds has allowed for the discovery of a new class of porous materials. Preliminary results show the ability to obtain porous, crystalline supramolecular boronate networks from the coordination of diamine linkers with boronate diester backbones. Further exploration of porous, crystalline supramolecular boronates has revealed the discovery of a porous crystalline coordination polymer that exhibits reversible, selective guest adsorption properties towards benzene. Our studies have also lead to the discovery of a system that undergoes solvent induced polymorphic behavior resulting in optical transitions for the development of a benzene sensing material. Finally, the discovery of several new crystalline, porous supramolecular boronate inclusion compounds has been achieved through variation of reaction solvent and or modification of the initial building blocks used to construct the network.

Table of Contents

List of Tables

List of Figures

List of Abbreviations

1,2-dpe ..... 1,2-di-(4-pyridyl)ethylene

1-D 1-Dimensional

^{1}H NMR ..... Proton Nuclear Magnetic Resonance

2-D 2-Dimensional

3-D 3-Dimensional

4,4'-bpy ..... 4,4'-bipyridine

B-N ..... Boron-Nitrogen

BTEX ..... Benzene, Toluene, Ethylbenzene, Xylenes

CIF ..... Crystallographic Information File

COF ..... Covalent Organic Framework

DSC ..... Differential Scanning Calorimetry

MOF ..... Metal Organic Framework

PXRD ..... Powder X-ray Diffraction

SMB ..... Supramolecular Boronate

STP ..... Standard temperature and pressure

TGA ..... Thermogravimetric Analysis

VOC ..... Volatile Organic Compound

XRD ..... Single Crystal X-ray Diffraction

Chapter 1 Introduction

1.1 Overview

The discovery of new, porous materials continues to be of high interest due to the demands of our ever growing and technologically advancing society. Over the past few decades, researchers have been developing new microporous materials such as coordination polymers or metal organic frameworks, zeolites and covalent organic frameworks for a wide variety of applications. In fact, the last two decades has seen enormous research efforts in the syntheses and studies of coordination polymers and thus the field of coordination polymers continues to expand exponentially.[1] The synthesis of new coordination polymers has provided a variety of properties ranging from storage, separation and exchange of guests in their cavities, to magnetism, conductivity and catalysis by such frameworks.[2] Many of these coordination polymers are logically constructed from molecular building blocks to yield crystalline porous materials in which metal ions and clusters are link by organic units, but the ability to assemble covalently linked coordination networks could lead to a generation of more structurally stable assemblies.[3] Researchers have recently developed a new class of coordination polymers known as covalent organic frameworks which are based on reversible boronate ester formation between boronic acids and diols or molecular dehydration reactions of benzene diboronic acid to create porous, crystalline frameworks solely from light elements.[4] More recently, researchers have developed supramolecular boronate (SMB) coordination polymers that rely on the dative boron-nitrogen (B-N) interaction in conjunction with

boronate ester formation.[5] We have developed porous, crystalline SMB networks that act as hosts to molecular guest such as benzene, toluene, xylenes and other benzene derivatives. These networks exhibit interesting guest adsorption properties and solvent induced polymorphism with associated optical properties that could be used for benzene sensing applications.

1.2 Background

Microporous materials have been commercially available for years, one specific type being zeolites for their applications in petrochemical cracking, softening and purification of water, separation of gases, and chemical absorbents.[6] In the early 1990s research on a new class of crystalline, porous materials know as metal organic frameworks (MOFs) took off and has been an ever growing field since. Like zeolites, MOFs are porous and crystalline, but unlike zeolites they are not purely inorganic compounds. MOFs are constructed of metal atoms or clusters called nodes which are connected by organic ligands called linkers to form 1D, 2D, or 3D networks. MOFs have received tremendous attention over the past years due to the fact that they can be made porous, have large surface areas and tunable pore sizes and topologies, all which lead to versatile architectures and promising applications such as ion exchange, adsorption, separation processes, drug delivery, sensor technology, catalysis, luminescence, host for polymerization reactions, magnetism, and non-linear optics (**Figure 1.1**).[7]

Conventional porous coordination polymers are generally rigid 3-D frameworks, but more recent advances has shown the construction of flexible porous coordination polymers where the flexible, porous properties has allowed for highly selective guest accommodation due to the dynamic nature of such structures. Adding flexibility to

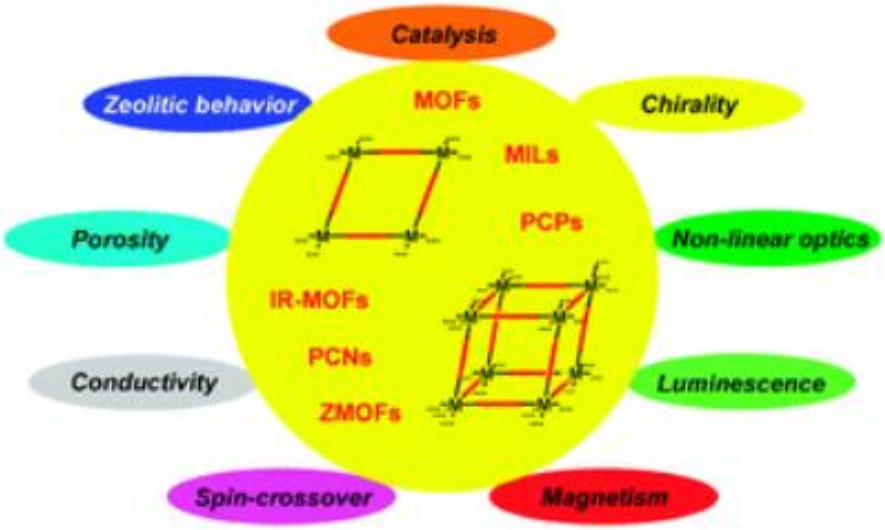

Figure 1.1: Schematic presentation of MOF structures form 1D-3D with common linkers shown inside the yellow circle surrounded by application oriented properties that make MOFs of great interest to researchers.

porous coordination polymers could help develop a unique class of materials that undergo dynamic structural transformations that cannot be obtained by rigid porous materials.[2] These flexible porous networks have been coined 3rd generation microporous coordination polymers and are subdivided into three types as shown in **Figure 1.2**.[8]

Type-I is known as the "recoverable collapsing" framework which, upon removal of guest the network collapses due to close packing forces, however it regenerates under the initial conditions. Type-II is known as the "guest-induced transformation" network because it will undergo structural shifts upon simultaneous exchange of guest molecules. Finally, type-III is known as the "guest-induced reformation" network because removal of guests causes a structural change of the network, however exposure to initial conditions results in reformation of the starting network.[2]

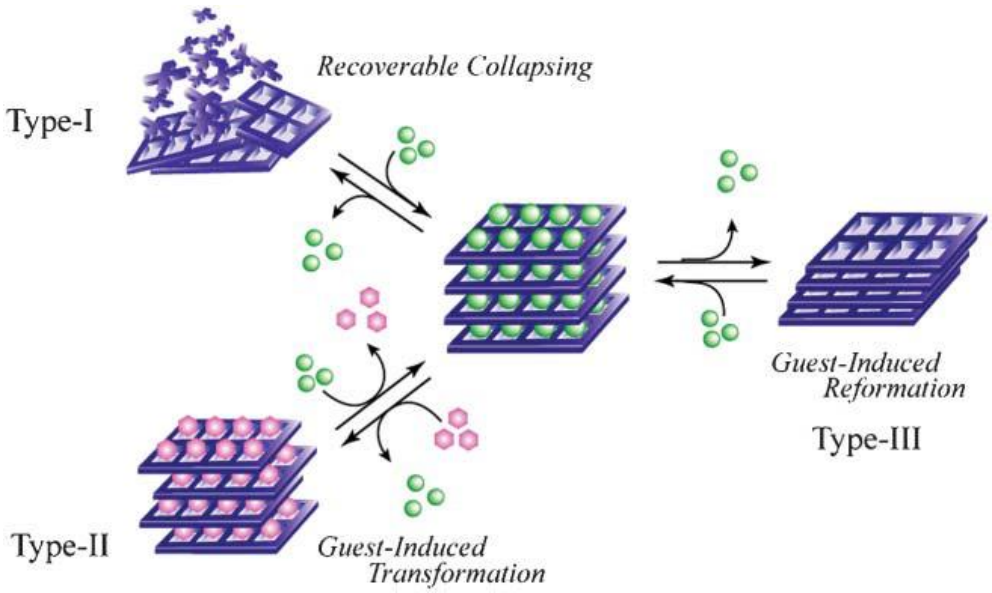

Figure 1.2: Schematic representation of the three types of 3rd generation microporous coordination polymers.

An interesting example of a type-II flexible microporous coordination polymer is the nickel based network $\{[Ni(L)_2(NO_3)_2]\cdot 4(o\text{-xylene})\}_n$ where L=4,4'-bis(4-pyridyl)biphenyl, which exhibits sliding of its 2-D grids upon guest exchange from ortho-xylenes to mesitylene as shown in **Figure 1.3**.[9] This guest exchange induced structural transformation is reversible and carried out without loss of single crystallinity. The initial network contains 2-D layers that are formed by square grids that are occupied by 4 ortho-xylene molecules per unit. Exchange of the ortho-xylene guests with mesitylene guests results in sliding of the 2-D grids which expands the pores now occupied by 1.7 mesitylene molecules per unit.

Another interesting example of a flexible porous coordination polymer is the cobalt based network $\{[Co(NCS)_2(4\text{-peia})_2]\cdot 4Me_2CO\}_n$ where 4-peia=N-(2-pyridin-4-yl-ethyl)-isonicotinamide, which exhibits type-I properties of collapsing to an amorphous form upon guest removal as shown in **Figure 1.4**.[10] The researchers reported that this

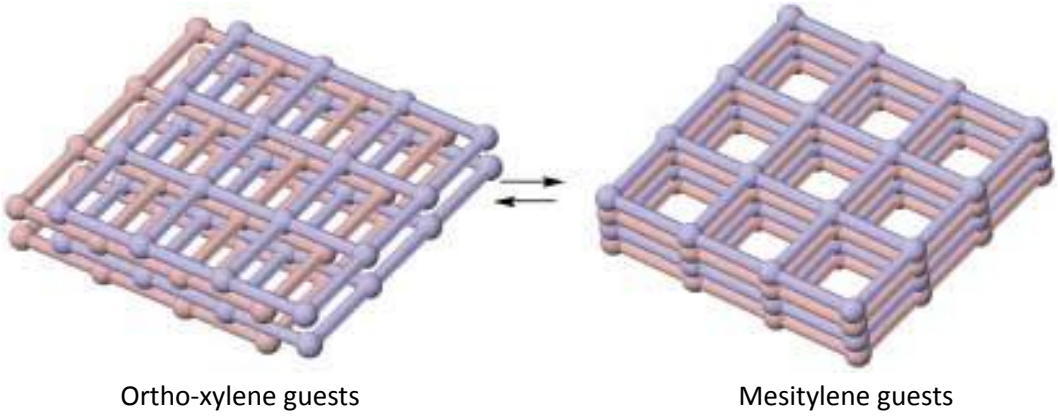

Figure 1.3: Schematic representation of sliding of the 2-D grids induced by guest exchange from ortho-xylene to mesitylene.

framework cannot withstand the high level of stress accompanied by extensive loss of the acetone guest which results in an amorphous form of the network. Interestingly, upon exposure to acetone vapor, the original crystal structure completely regenerates indicating the importance of the acetone guest for structural support of the network. The reversible nature of boronate ester bonds along with dative B-N coordination bonds may be promising for constructing SMB coordination networks that exhibit porous, flexible behavior accompanied with unique guest adsorption properties.

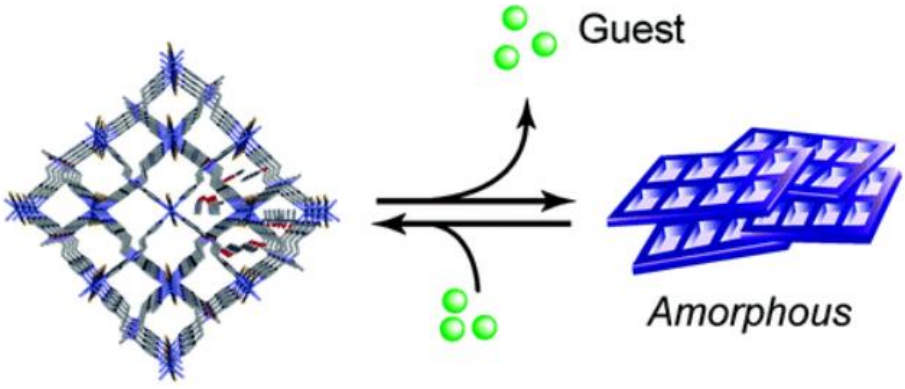

Figure 1.4: Schematic representation of structural transformation from a porous, crystalline host network occupied by acetone guests to an amorphous network upon removal of the guest. This process was shown to be reversible where exposure to acetone vapor causes regeneration of the initial crystalline, porous framework.

Boron is a truly unique element, considered a metalloid having properties that are intermediate between metals and nonmetals. Neutral boron is a tri-coordinate element containing an empty p-orbital and thus most boron containing species act as Lewis acids, coordinating to Lewis bases. As such, the SMB assemblies discussed in chapters 2, 3 and 4 are linked by B-N dative bonds in which the lone pair of electrons on an amine coordinates with the empty p-orbital on the boron centers affording a tetrahedral geometry on the boron.[11,12,13] The use of bi-functional amines leads to the formation of extended structural networks. Crystalline supramolecular boronates represent a class of porous coordination materials with promising applications in molecular sensing, gas storage and with possible environmental remediation capabilities[14].

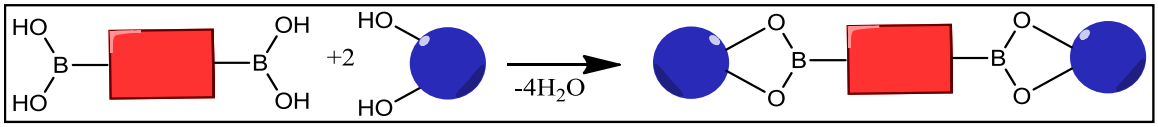

Figure 1.5: Schematic of the dehydration reaction between diboronic acids and diols

Supramolecular boronates or boronate diester coordination materials consist of boronate diester backbones formed through the dehydration reaction between a diboronic acid and a 1,2- or 1,3-diol (**Figure 1.5**). A diamine linker is then added and the lone pair on the nitrogen coordinates with the empty p-orbital of boron forming B-N dative bonds (**Figure 1.6**). Related polymeric coordination networks exhibiting intrastrand charge-transfer excitations has been previously reported using boronic acids and 1,2,4,5-tetrahydroxy benzene[15]. The reversible nature of the B-N dative bonds allows for the formation of highly crystalline materials with extended long range order.

The use of the unique covalent yet reversible boronate ester bonds alone or in conjunction with the dative B-N coordination bonds has been employed for construction

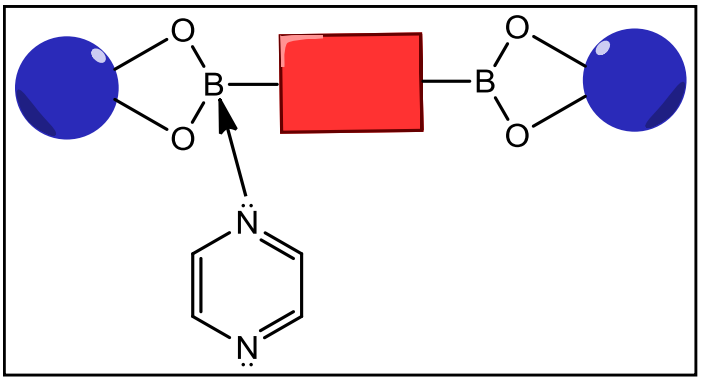

Figure 1.6: Cartoon schematic representation of a boron-nitrogen dative bond. The lone pair of electrons on the nitrogen is donated into the empty p-orbital on the boron creating a weak reversible coordination bond.

of crystalline, porous covalent organic frameworks, linear self-repairing polymers, macrocycles, cages, and other SMB networks.[16,17,18,19] One example of the use of boronate ester and B-N dative bonds to form a macrocycle is shown in **Figure 1.7** in which this macrocycle has a calix[3]arene-like shape and is able to act as a host for primary amines and ammonium chlorides with binding constants in the range of 10^2-10^3 M^{-1} in methanol.[17]

Generally when a porous, crystalline macrocycle or framework is constructed the void space is occupied by a solvent of crystallization. The interactions between the network and the solvent can play a large role in the structural integrity of the network, causing the network to collapse upon removal of the guest solvent. Constructing networks that maintain structural integrity upon removal of guest is of interest for applications in gas storage and selective guest adsorption or exchange. Our work focuses on the construction of porous, crystalline SMB networks that act as host networks to benzene and its derivatives while exhibiting selectivity and possible optical transitions for use in sensing applications.

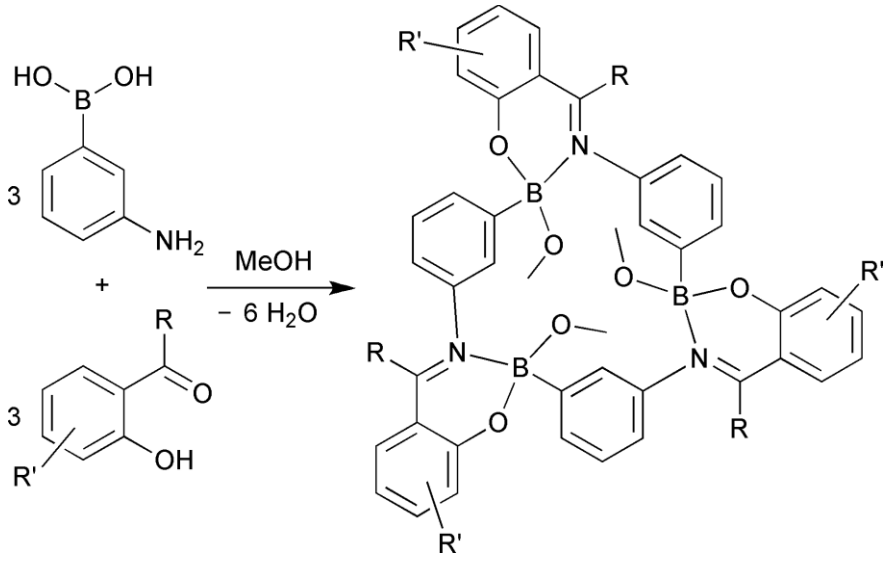

Figure 1.7: Synthetic scheme for the formation of trimeric macrocycles from the condensation reactions of 3-aminophenylboronic acid with substituted salicylaldehydes.

1.3 References

[1] Janiak, C. Engineering Coordination Polymers Towards Applications. *Dalton Trans.* **2003**, 2781-2804.

[2] Uemura, K.; Matsuda, R.; Kitagawa, S. Flexible Microporous Coordination Polymers. *Journal of Solid State Chemistry.* **2005**, *178*, 2420-2429.

[3] Tilford, R. W.; Gemmil, W. R.; zur Loye, H.-C.; Lavigne, J. J. Facile Synthesis of a Highly Crystalline, Covalently Linked Porous Boronate Network. *Chem. Mater*. **2006**, *18*, 5296-5301.

[4] Cote, A. P.; Benin, A. I.; Ockwig, N. W.; O'Keeffe, M.; Matzger, A. J.; Yaghi, O. M. Porous, Crystalline, Covalent Organic Frameworks. *Science.* **2005**, *310*, 1166-1170.

[5] Rambo, B. R.; Tilford R. W.; Lanni, L. M.; Liu, J.; Lavigne, J. J. Boronate-Linked Materials: Ranging from Amorphous Assemblies to Highly Structured Networks. In *Macromolecules Containing Metal and Metal-like Elements*, Abd-El-Aziz, A. S.; Carraher Jr., C. E.; Pittman Jr., C. U.; Zeldin, M. Ed. John Wiley & Sons, Inc.: Hoboken, New Jersey, 2009; Vol. 9, pp 255-294.

[6] Reinhold, C. Metal-Organic Frameworks Take on New Structure: Porous Materials. *Mater. Today.* **2007**, *10*, 10.

[7] Janiak, C.; Vieth, J. K. MOFs, MILs and More: Concepts, Properties and Applications for Porous Coordination Networks (PCNs). *New J. Chem.* **2010**, *34*, 2366-2388.

[8] Kitagawa, S.; Uemura, K. Dynamic Porous Properties of Coordination Polymers Inspired by Hydrogen Bonds. *Chem. Soc. Rev.* **2005**, *34*, 109-119.

[9] Biradha, K.; Hongo, Y.; Fujita, M. Crystal-to-Crystal Sliding of 2D Coordination Layers Triggered by Guest Exchange. *Angew. Chem. Int. Ed.* **2002**, *41*, 3395-3398.

[10] Uemura, K.; Kitagawa, S.; Fukui, k.; Saito, K. A Contrivance for a Dynamic Porous Framework: Cooperative Guest Adsorption Based on Square Grids Connected by Amide-Amide Hydrogen Bonds. *J. Am. Chem. Soc.* **2004**, *126*, 3817-3828.

[11] Liu, J.; Lavigne, J. In *Boronic Acids: Preparation and Applications in Organic Synthesis, Medicine and Materials;* 2nd Ed. Hall, D., Ed.; Wiley-VCH: Weinheim, Germany, 2011; Vol. 2, pp 621-676.

[12] Sheepwash, E.; Krampl, V.; Scopelliti, R.; Sereda, O.; Neels, A.; Severin, K. *Angew. Chem. Int. Ed.* **2011,** *50*, 3034-3037.

[13] Icli, B.; Sheepwash, E.; Riss-Johannessen, T.; Schenk, K.; Filinchuk, Y.; Scopelliti, R.; Severin, K. *Chem. Sci.* **2011,** *2*, 1719-1721.

[14] Nishiyabu, R.; Kubo, Y.; James, T.; Fossey, J. *Chem. Commun.* **2011,** *47*, 1124-1150.

[15] Christinat, N.; Croisier, E.; Scopelliti, R.; Cascella, M.; Rothlisberger, U.; Severin, K. *Eur. J. Inorg. Chem.* **2007,** 5177-5181.

[16] Niu, W.; O'Sullivan, C.; Rambo, B. M. Smith, M. D.; Lavigne, J. J. Self-Repairing Polymers: Poly(dioxaborolane)s Containing Trigonal Planar Boron. *Chem. Commun*. **2005**, 4342-4344.

[17] Severin, K. Boronic Acids as Building Blocks for Molecular Nanostructures and Polymeric Materials. *Dalton Trans.* **2009**, 5254-5264.

[18] Christinat, N.; Scopelliti, R.; Severin, K. Multicomponent Assembly of Boronic Acid Based Macrocycles and Cages. *Angew. Chem. Int. Ed.* **2008**, *47*, 1848-1852.

[19] Fujita, N.; Shinkai, S.; James, T. D. Boronic Acids in Molecular Self-Assembly. *Chem. Asian J.* **2008,** *3*, 1076-1091.

Chapter 2 Supramolecular Boronate Coordination Polymer

2.1 Overview

Boronate esters represent a class of materials that exhibit covalent yet reversible bonding interactions that allow for desirable self-assembling materials with dynamic self-repairing capabilities.[1] The ability to generate porous, robust materials in an efficient and simple manner is greatly desired for applications in gas storage, catalysis, separations, sensing, and molecular sequestration.[2] Boronate esters are Lewis acids that can form dative bonds to N-donor ligands in which the nitrogen donates its lone pair of electrons to the empty p-orbital on the boron. B-N dative bonds between ditopic N-donor ligands and boronate esters have been employed for construction of supramolecular networks such as macrocycles and linear polymers.[3] The reversible nature of the B-N dative bonds allows for the formation of highly crystalline materials with extended long range order.

The Severin group successfully synthesized a new type of coordination polymer utilizing boronate esters and bipyridine linkers that exhibits interesting optical transitions through intrastrand charge transfer transitions (**Figure 2.1**).[4] Further exploration of this new class of coordination polymers by the Lavigne group has led to the discovery of new porous supramolecular boronates (SMBs) that show the ability to store, adsorb and sense benzene derivatives.

2.2 Synthesis of Supramolecular Boronate Coordination Polymer from Benzene

The Lavigne group has previously shown that boronate esters formed from condensation reactions between boronic acids and diols can be used to form porous

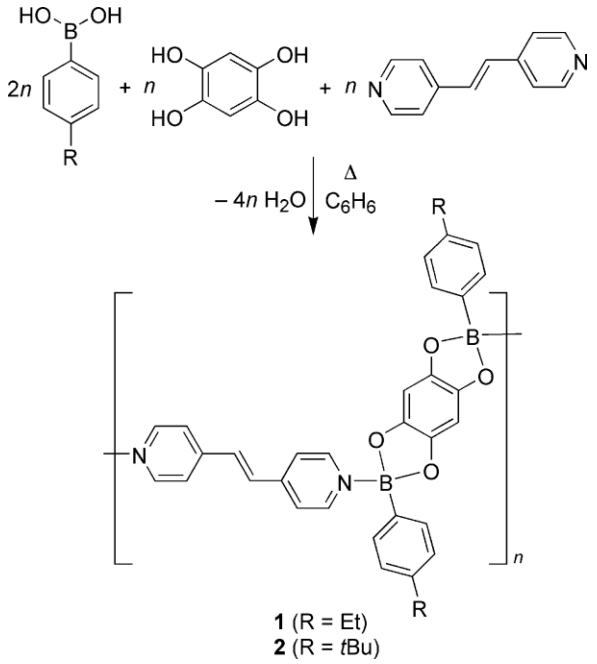

Figure 2.1: Severin group SMB coordination polymer single-pot synthesis from substituted phenyl boronic acid, tetrahydroxybenzene and 1,2-di-(4-pyridyl)ethylene

materials such as covalent organic frameworks (COFs) and self-assembling linear boronate esters.[2, 5] Utilizing the empty p-orbital on boron and hence the Lewis acidity of the boronate esters, we incorporated diamine linkers to produce SMB porous materials where the boronate ester backbones are linked by diamine ligands through B-N dative bonds.

The first SMB material discovered by the Lavigne group incorporated 9,9-dihexylfluorene-2,7-diboronic acid, catechol and 1,2-di-(4-pyridyl)ethylene (1,2-dpe) reacted in refluxing benzene, providing a facile synthesis which can be performed as a single-pot reaction or a two-step reaction to yield **compound 2.1** as shown in **Figure 2.2**. Upon undisturbed slow cooling of the solution, clusters of single crystal X-ray diffraction (XRD) quality crystals are obtained in high yield (**Figure 2.3**).

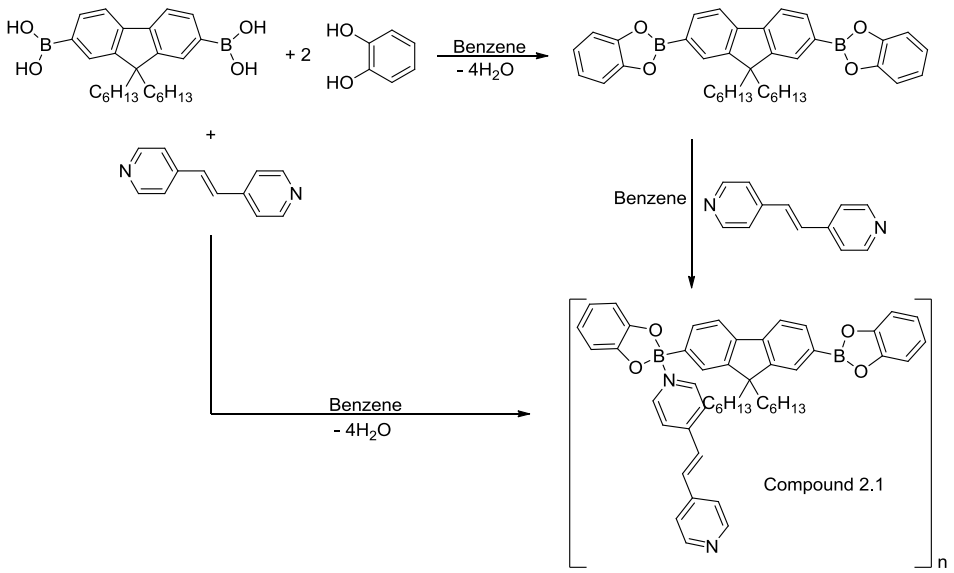

Figure 2.2: Synthetic scheme for **compound 2.1** shown as single pot and two step reaction. In the two step reaction method 9,9-dihexylfluorene-2,7-diboronic acid and catechol undergo a condensation reaction to form a boronate diester before coordination with 1,2-di-(4-pyridyl)ethylene to form **compound 2.1**. In the single-pot synthesis B-N coordination occurs in conjunction with the condensation reaction to yield **compound 2.1**.

Single crystal XRD analysis reveals that **compound 2.1** crystallizes in the monoclinic space group $P2_1/n$ as determined uniquely by the pattern of systematic absences in the intensity data. The asymmetric unit consists of one $[(C_{37}H_{40}B_2O_4)(C_{12}H_{10}N_2)]$ polymeric complex, half each of two benzene molecules located on inversion centers, and another complete benzene molecule giving **compound**

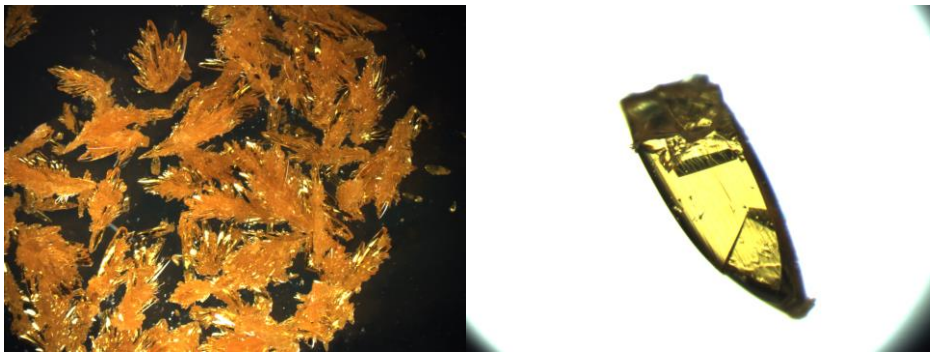

Figure 2.3: Compound 2.1 orange crystal clusters (left) as seen by the naked eye. Pale yellow single crystal of **compound 2.1** (right) observed at 11X zoom on an optical microscope

2.1 a molecular formula of $[(C_{37}H_{40}B_2O_4)(C_{12}H_{10}N_2)]\cdot 2(C_6H_6)$. Infinite 1-D polymeric chains (**Figure 2.4a**) running along the crystallographic b-axis are composed of $C_{37}H_{40}B_2O_4$ molecules linked by $C_{12}H_{10}N_2$ spacers. C_6H_6 molecules fill the voids left between the packing of the chains (**Figure 2.4b**).

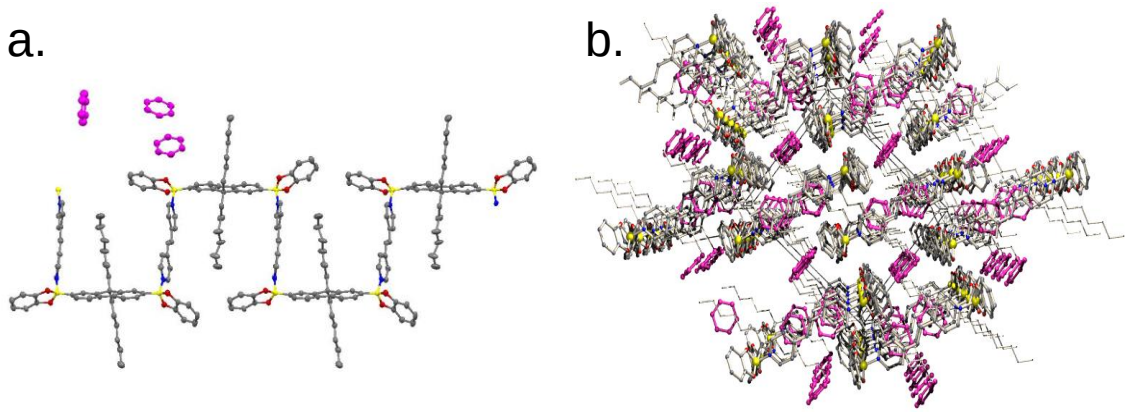

Figure 2.4: a. Connectivity of the 1-D chains of **compound 2.1**. The diamine linkers are connected to the boronate diester backbone in a cis fashion creating square zigzag chains. **b.** Crystallographic packing of the 1-D chains of **compound 2.1** viewed down the crystallographic b-axis. Benzene guest molecules are shown in purple and occupy the void space between the packing of the 1-D polymeric chains.

2.3 Benzene Inclusion Properties of Compound 2.1

The structural analysis via single crystal XRD revealed that **compound 2.1** is an inclusion compound that acts as a host to benzene guest molecules which constitute about 17.2% of the mass of the network. Calc. SOLV in Platon was performed on **compound 2.1** after removing benzene from the crystallographic information file (CIF), revealing a total potential solvent accessible void of 1204.7$Å^3$ per unit cell volume, constituting 23.9% of the total crystal volume.[6] The benzene guest molecules are held tightly by the network evidenced by thermogravimetric analysis (TGA) which shows that the release of benzene from the network occurs at about 110°C which is 30°C above the boiling point of benzene at STP (**Figure 2.5a**). Further evidence of the strong benzene-host interaction

is that after one week under reduced pressure (1mm Hg) at ambient temperature about 30% of the benzene is still present in the network (**Figure 2.5a inset**). It is expected that the benzene is held tightly through multiple CH/π interactions between the host network and the benzene guest, as well as other weak intermolecular interactions.

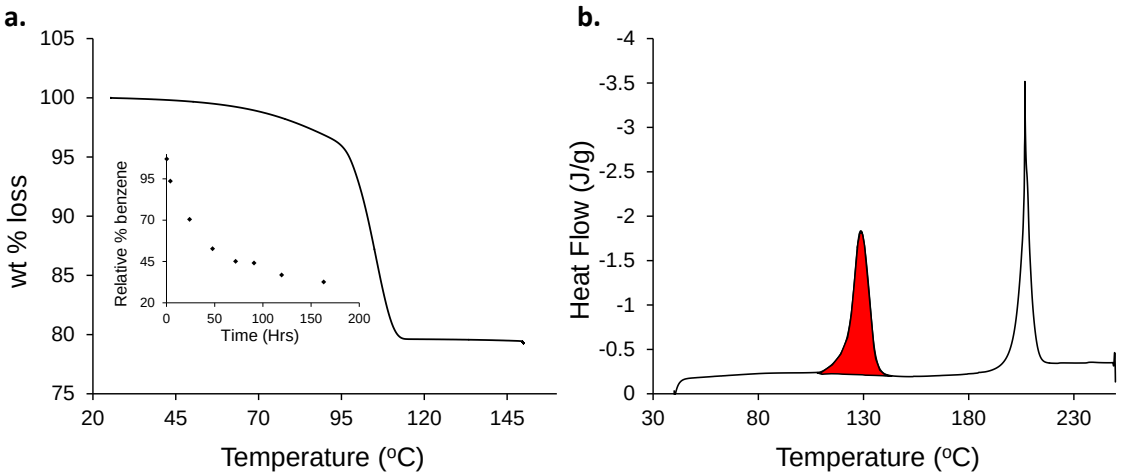

Figure 2.5: a. TGA plot of **compound 2.1** shows the weight % loss associated with the removal of benzene. The sharp drop in the plot around 110°C represents the loss of benzene from the network. **Inset.** Graph showing the relative % benzene in **compound 2.1** verse time under vacuum at ambient temperature. It can be seen that reduced pressure alone is not enough to completely remove benzene from **compound 2.1** in a timely manner. **b.** DSC trace of the initial heat ramp of **compound 2.1**. Integration of red area = ΔH_{sexp} and is used to calculate the strength of the interaction between **compound 2.1** and the benzene guest molecules.

The strength of host-guest interaction was determined through a combination of TGA and differential scanning calorimetry (DSC) thermal analysis. Integration of the endothermic peak corresponding to the loss of benzene in DSC gives the experimental enthalpy of desolvation per gram of solvate (ΔH_{sexp}) (**Figure 2.5b**). Using ΔH_{sexp} and the % mass loss (Δm_s%) obtained from TGA, the following equation can be used to calculate the enthalpy of desolvation (ΔH_s) or binding energy,

$$\Delta H_s = [(\Delta H_{sexp} \times 100)/ \Delta m_s\%] \times M_s$$

where M_s is the molecular mass of the solvent.[7] We have calculated a ΔH_s of 43.5 KJ/mol as compared to the standard enthalpy of vaporization ($\Delta H°_{vap}$) of benzene which is 33.9KJ/mol.[8] The difference between ΔH_s and $\Delta H°_{vap}$ gives us a $\Delta\Delta G$ of 9.55 KJ/mol or 2.28 Kcal/mol which allows us to put the strength of the host-benzene interaction in context with common intermolecular interactions. For example, a common CH/π interaction has the strength of about 1.5-3 Kcal/mol and the π/π stacking of benzene in the gas phase has the strength of about 2-3 Kcal/mol.[9,10] Based on the calculated strength of our host-guest interaction, it is fair to say that CH/π interactions between the benzene guest and **compound 2.1** are consistent with expected values.

2.4 Structural Determination of Desolvated Compound 2.1

Despite the strong interaction between **compound 2.1** and the benzene guest molecules we have shown that the benzene can still be removed from the network. Removal of benzene is accompanied by a loss of single crystallinity, but Powder X-ray Diffraction (PXRD) analysis of desolvated **compound 2.1** indicates that the removal of benzene is not accompanied by a complete loss of crystallinity. It is also clear from the PXRD analysis of desolvated **compound 2.1** that the loss of benzene is accompanied by a change in the unit cell of the network as evidenced in the difference in PXRD patterns between the solvated and desolvated forms of **compound 2.1** (**Figure 2.6**).

It is expected that upon removal of the benzene guest molecules the network undergoes a shrinkage or compression of the voids between the packing of the 1-D polymeric chains where the benzene molecules were once residing. To support this hypothesis, we performed a LeBail or full profile refinement of the PXRD pattern of

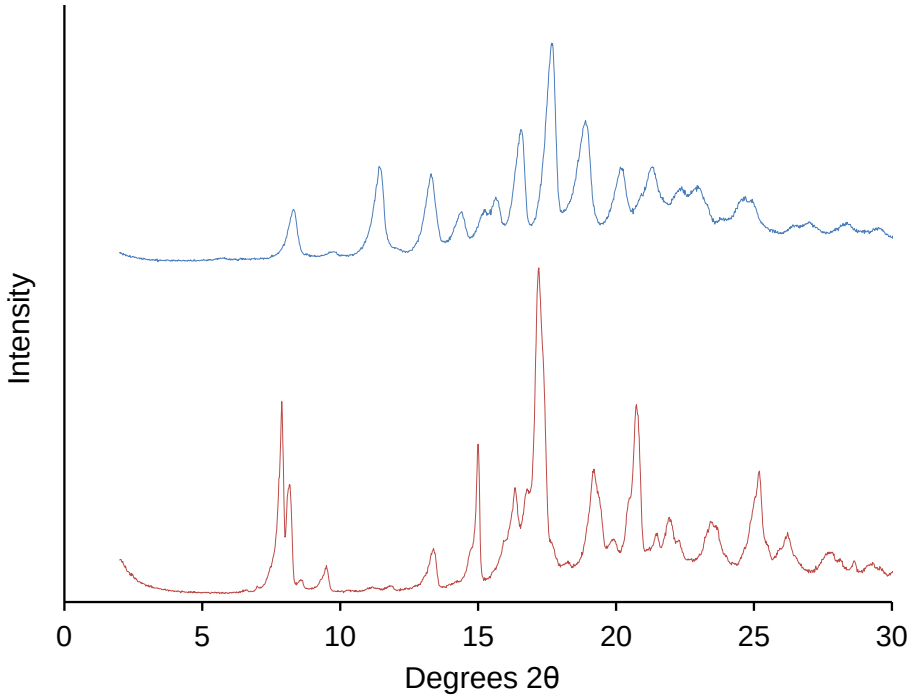

Figure 2.6: PXRD pattern of crystals of solvated **compound 2.1** shown in red. PXRD pattern of desolvated **compound 2.1** shown in blue. It is clear that the PXRD patterns of the solvated (red) and desolvated (blue) forms of **compound 2.1** are different.

desolvated **compound 2.1** using the EXPGUI interface to the GSAS software.[11,12] The refinement calculates the goodness of fit or χ^2 between a calculated pattern determined from the newly refined unit cell parameters and peak shape to the observed or experimental pattern. The LeBail fit of desolvated **compound 2.1** was completed with χ^2 = 9.995 and the calculated, observed and difference patterns from the refinement are shown in **Figure 2.7**. The starting unit cell parameters for the refinement were determined by indexing the powder pattern with JADE. The newly determined unit cell parameters of desolvated **compound 2.1** are shown in **Table 2.1** along with the unit cell parameters of solvated **compound 2.1** as determined from single crystal XRD. Comparison of the two unit cells clearly shows that removal of the benzene guest from **compound 2.1** is accompanied by shrinkage of the unit cell.

Table 2.1: Unit cell dimensions of solvated **compound 2.1** from single crystal XRD analysis and desolvated **compound 2.1** from the LeBail fit of the PXRD pattern.

Compound	**Compound 2.1 solvated**	**Compound 2.1 desolvated**
Space group	Monoclinic $P2_1/n$	Monoclinic $P2_1/c$
a (Å)	13.8584	9.0158
b (Å)	21.5582	15.6151
c (Å)	16.9252	14.9687
β (°)	95.648	98.572
Vol. (Å^3)	5032.1	2083.8

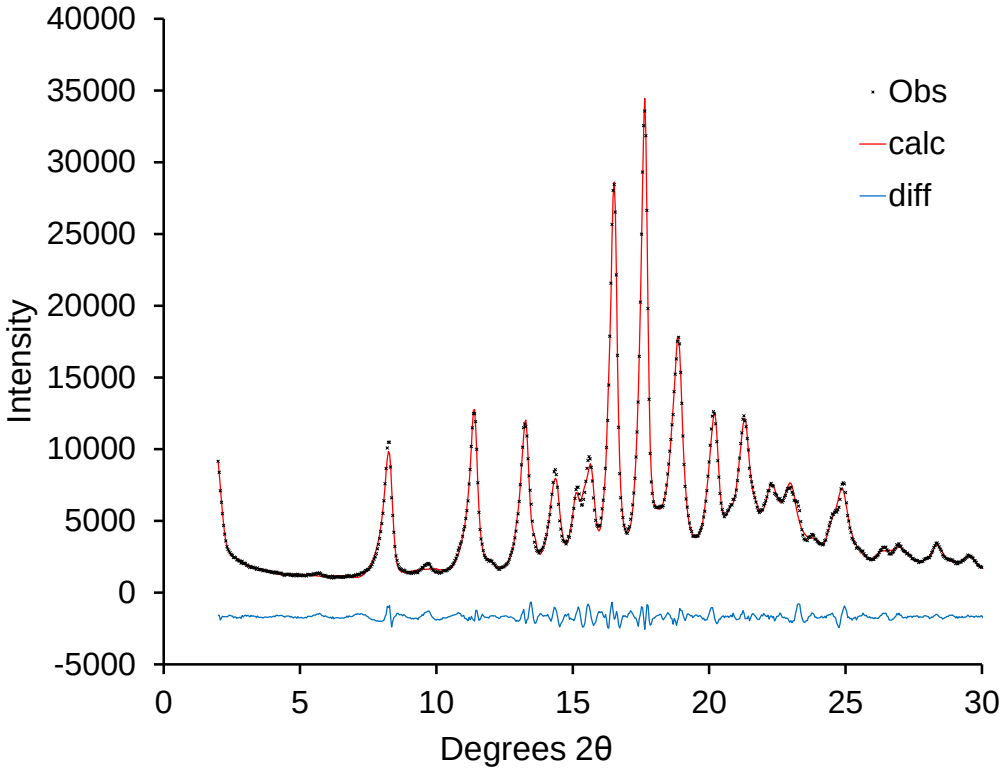

Figure 2.7: Results of LeBail fit of the PXRD pattern of desolvated **compound 2.1**. The black x's are the observed or experimental PXRD pattern of desolvated **compound 2.1** and the red line is the calculated PXRD pattern from the newly refined unit cell parameters and peak shape. The blue line at the bottom is a plot of the difference between the observed and calculated patterns. The refinement was completed with $\chi^2 = 9.995$ which represent the goodness of fit.

2.5 Isolation Method Study of Compound 2.1

Other studies have shown that the method upon which **compound 2.1** is isolated affects the crystallinity of the porous network and thus guest retention and removal. For example, when the refluxing solution is allowed to cool slowly without disturbance, XRD quality single crystals grow within days, whereas if the solution is isolated by rotary evaporation a microcrystalline powder is obtained. When analyzing the two products for benzene retention we observed that the crystals tend to retain slightly more benzene than the powder, but the difference is not large and the powders isolated by rotary evaporation still retain more than 85% of the theoretical benzene retention. When comparing benzene removal from the crystalline material, **Figure 2.8** shows a clear difference in TGA curve shape of the crystals compared to the powder.

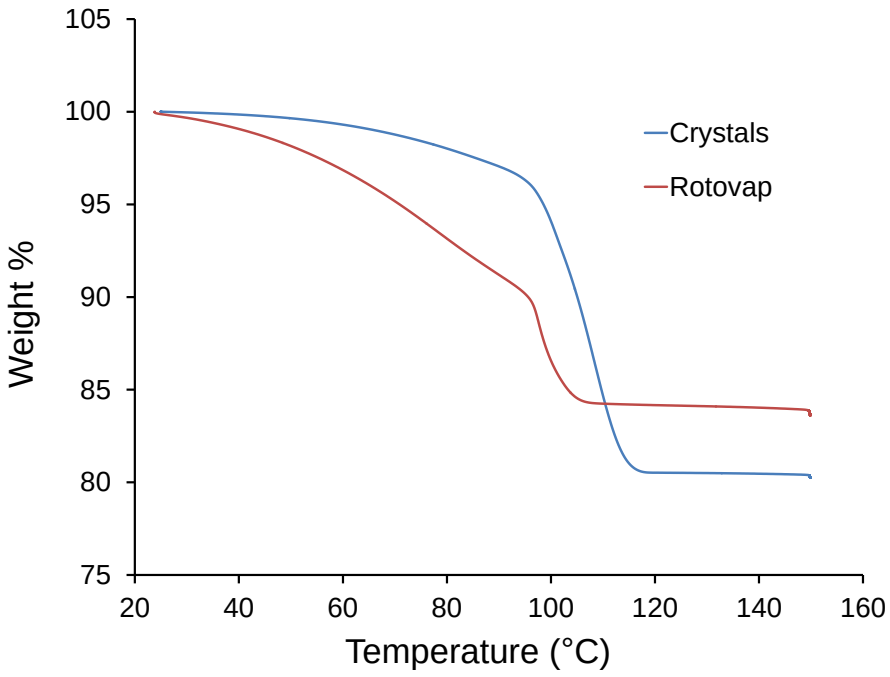

Figure 2.8: TGA plot of crystals of **compound 2.1** (blue) shown along with a TGA plot of rotary evaporated powder of **compound 2.1**(red). It is clear from the two plots that crystals of **compound 2.1** retain more benzene and hold onto the benzene to a higher temperature than the rotary evaporated powder of **compound 2.1**.

My hypothesis for the observed difference is that the crystals have a higher degree of long range order and thus the channels extend deep into the structure trapping the benzene guest molecules which are not released until well above their boiling point of 80°C. The powder has more surface area and a lower degree of long range order so the channels are closer to the surface resulting in easier release of the benzene guest molecules.

2.6 Benzene Reloading Methods for Compound 2.1

We have shown that **compound 2.1** is a benzene inclusion compound upon which benzene can be removed without destruction of the network. This prompted the question, can **compound 2.1** re-adsorbed benzene? It was found that upon soaking desolvated **compound 2.1** in liquid benzene that the network re-adsorbs benzene, regenerating the original benzene solvated **compound 2.1** confirmed by PXRD of the as synthesized and reloaded **compound 2.1** (**Figure 2.9**). Desorption/adsorption cycles of benzene can be repeated several times showing us the ability of this material to act as a molecular sponge towards benzene. These results prompted studies of benzene reloading methods, time, and recoverability.

Several adsorption methods have been carried out to help determine the degree of benzene adsorption over time and the recoverability of the material under different reloading conditions. **Compound 2.1** was soaked in liquid benzene at several time intervals from 30 minutes to 24 hours. Analysis by ^{1}H NMR and TGA shows **compound 2.1** reloads to capacity within 24 hours. Exposure of desolvated **compound 2.1** to benzene vapor for 72 hours indicated that benzene adsorption occurs exclusively in the liquid phase. The general method for reloading desolvated **compound 2.1** is to put the

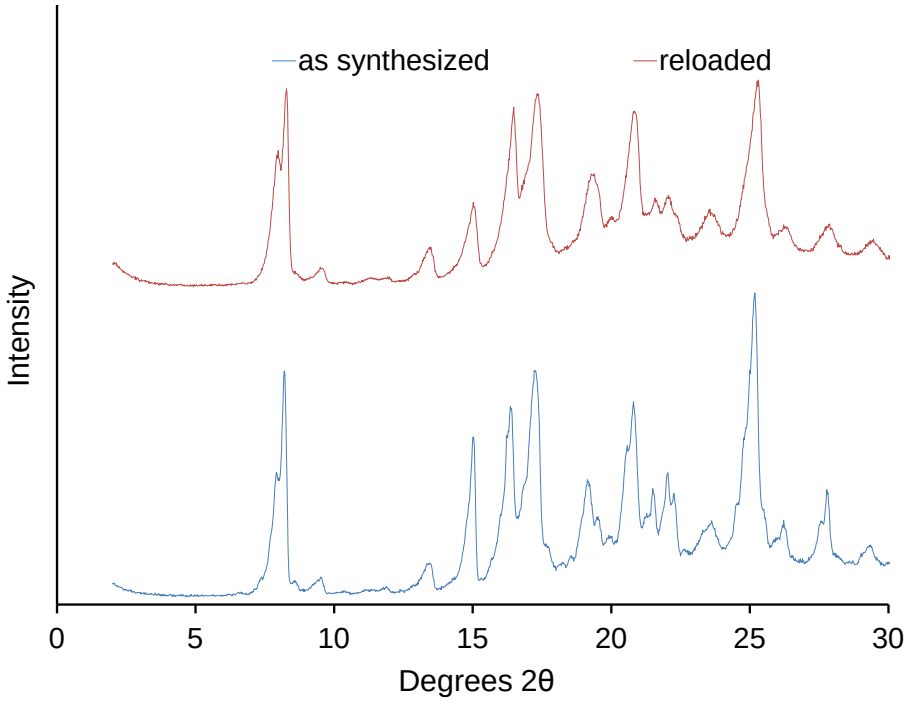

Figure 2.9: PXRD pattern of as synthesized **compound 2.1** (blue) and reloaded **compound 2.1** (red). Inspection of the two PXRD patterns confirms that immersion of desolvated **compound 2.1** in benzene results in regeneration of the initial solvated **compound 2.1**.

product in a vial, add about 2mL of liquid benzene, seal the vial and let sit undisturbed for 24 hours. This method was compared to three other methods (see experimental) which involved agitation while soaking to determine the effects on adsorption and recoverability of the material. The results revealed that all methods worked to reload **compound 2.1** to full capacity within 3 hours with recoverability above 86% as shown in **Table 2.2**. This shows that **compound 2.1** has good structural integrity and can be recovered in high yield for reuse.

The unique reversible benzene adsorption properties, along with the porosity and strong host-guest interactions observed in this SMB coordination polymer prompted investigation of the adsorption properties toward other similar volatile organic compounds (VOCs), specifically benzene derivatives.

Table 2.2: Results from benzene reloading method study on **compound 2.1**.

Method	% benzene (TGA)	% Recovery
Normal undisturbed	17.0%	89.2%
Continual shaking	16.4%	94.9%
Coffee filter in stirring benzene	16.6%	88.5%
Membrane filter in stirring benzene	16.9%	100%

2.7 Solvent Adsorption Studies of Compound 2.1

We started by investigating toluene, ethylbenzene and xylenes, as these along with benzene make up the BTEX class of compounds which are widely found in petroleum products, notoriously known as contaminants of soil and groundwater, and known to have harmful effects on the human central nervous system and thus are highly regulated pollutants.[13] When desolvated **compound 2.1** was immersed in liquid toluene, ethylbenzene, and xylenes (mix of all isomers) respectively, it was found that none of these compounds were adsorbed by the network as evidenced by TGA and ^{1}H NMR (**Figure 2.10**). To further confirm the selectivity towards benzene out of the BTEX compounds, desolvated **compound 2.1** was immersed in an equal-volume mixture of BTEX compounds, upon which benzene was adsorbed while the other components were excluded as confirmed by ^{1}H NMR and TGA (**Figure 2.10**).

The unique selectivity towards benzene prompted further investigation of benzene adsorption abilities from varying concentrations of BTEX mixtures. BTEX solutions containing different ratios of benzene to the other BTEX components were prepared and soaks were performed at different time intervals between 1 and 7 days. The results shown in **Figure 2.11** indicate that benzene is selectively adsorbed to near full capacity

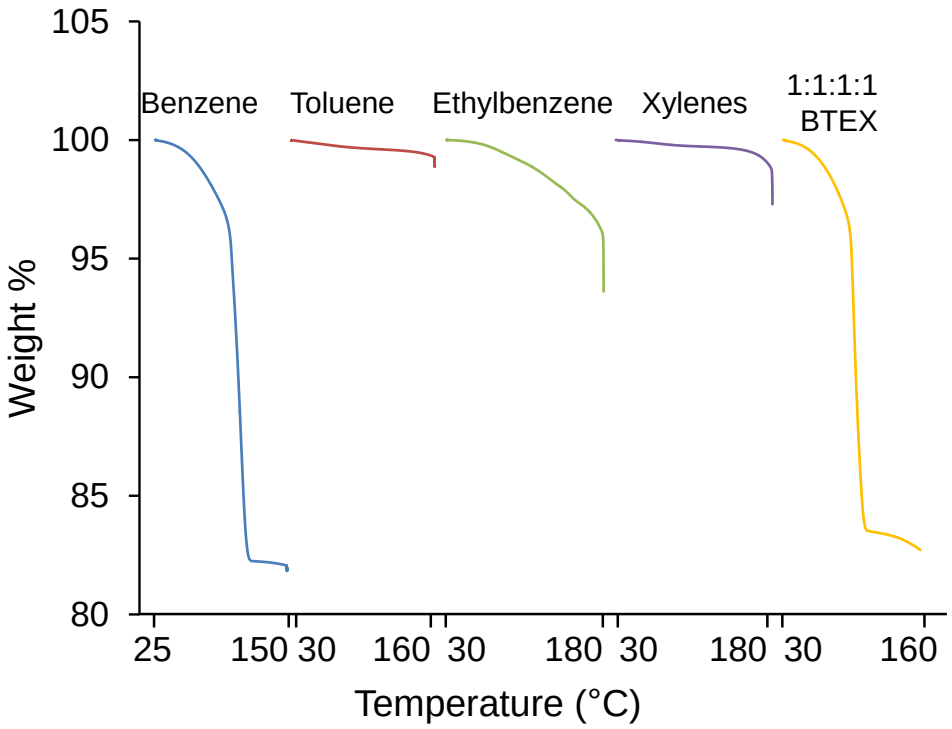

Figure 2.10: TGA plots taken after desolvated **compound 2.1** was soaked in the individual BTEX compounds and a 1:1:1:1 equal-volume mixture of BTEX compounds. The results show that desolvated **compound 2.1** only adsorbs benzene out of the class of BTEX compounds.

out of an equal-volume BTEX mixture within 24 hours, and that benzene is selectively adsorbed to partial capacity, increasing over time, out of a 0.5:1:1:1 volumetric BTEX mixture. Soaks using a 0.2:1:1:1 volumetric BTEX mixture did not adsorb any of the BTEX compounds, not even benzene. The ^{1}H NMR spectra do not contain toluene, ethylbenzene, or xylene peaks, further confirming selectivity for benzene.

The exclusion of the non-planar, sp^3 containing aromatic benzene derivatives toluene, ethylbenzene, and xylenes suggest that **compound 2.1** is selective towards planar aromatic guests. To further test this hypothesis, solvent adsorption studies were performed on several planar aromatic benzene derivatives of varying sizes including fluorobenzene, chlorobenzene, bromobenzene, iodobenzene, nitrobenzene, styrene

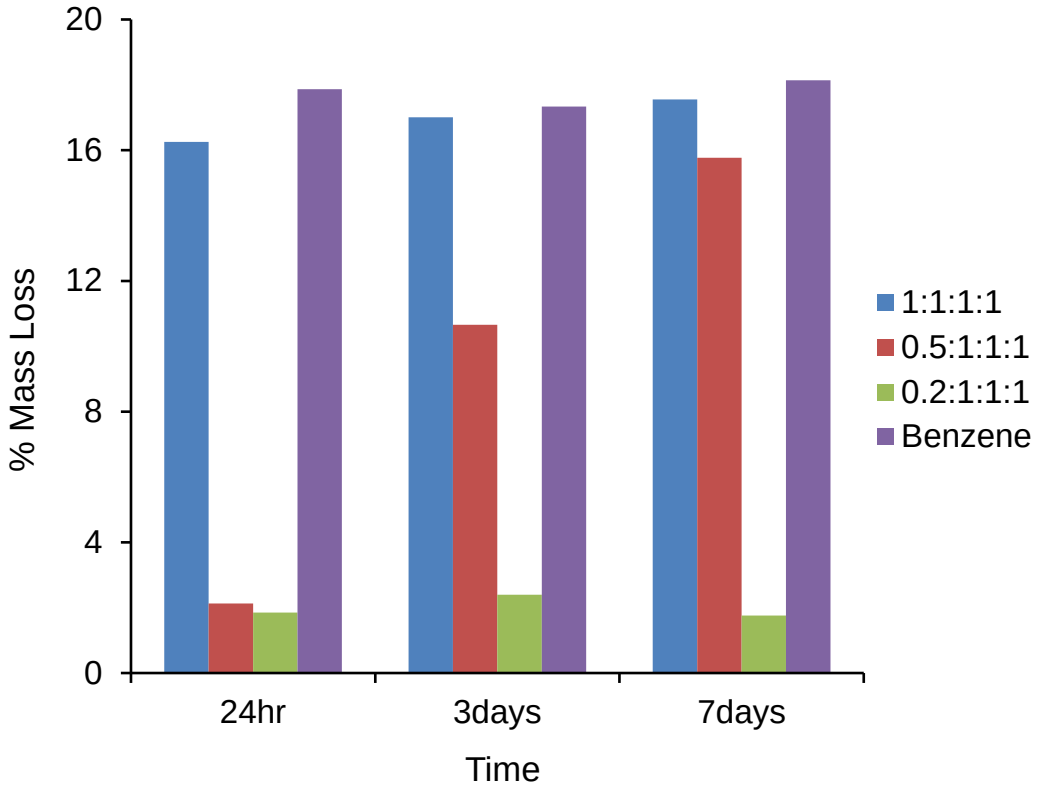

Figure 2.11: Bar graph showing the benzene % mass of the network adsorbed by desolvated **compound 2.1** when soaked in varying mixtures of BTEX compounds at different time intervals. Also shown is the benzene % mass of the network adsorbed by desolvated **compound 2.1** when soaked in benzene alone as a control.

and naphthalene. Of these seven planar, all sp^2 hybridized benzene derivatives only fluorobenzene, the smallest of all except benzene, was adsorbed as evidenced by TGA and ^1H NMR. Based on the results showing that **compound 2.1** only adsorbs benzene and fluorobenzene, we suggest that the network is not only specific towards adsorbing planar, all sp^2 hybridized aromatics, but is also size selective, excluding planar aromatic compounds with a longest intra-molecular distance of about 5.3Å or longer as determined by ChemBio3D Ultra 12.0.

2.8 Conclusion

In conclusion, we have discovered and studied a unique porous SMB coordination polymer that exhibits promising properties for potential applications in molecular storage,

sequestration, and sensing. We have shown that **compound 2.**1 has the ability to absorb benzene in a fairly selective and repeatable manner. We have also shown that the material is robust, recyclable, and easy to synthesize. Further studies on **compound 2.1** need to be performed to better evaluate its possible use for applications in molecular storage, sequestration, and sensing. The ability to process the material into films for sensing or into filters for benzene sequestration from water should be investigated to further understand the applicability of this SMB coordination polymer. **Compound 2.1** only represents one compound out of a potentially large class of compounds, some of which will be discussed in the following chapters.

2.9 Experimental

Synthesis of boronate diester: To a 500mL round bottom flask, 0.5016g (1.188 mmol) 9,9-dihexylfluorene-2,7-diboronic acid, 0.2761g (2.507 mmol) Catechol, and 250mL benzene were added. A Dean Stark trap with 3Å molecular sieves activated by heating under vacuum for 5 minutes and a reflux condenser was attached to the reaction flask. The initial murky white solution gave rise to a transparent solution after 30 minutes. The solution was refluxed overnight with stirring, under a nitrogen atmosphere at 110°C. The resultant clear solution was allowed to cool to room temperature. Benzene was removed by rotary evaporation, leaving behind a white solid. The product, a white solid was purified by reduced pressure sublimation (kugelrohr) for 4 hours at 115°C (0.6400g, 94.7% yield). ^{1}H NMR (300 MHz, CD_2Cl_2): δ 8.12-8.09 (m, 4H), 7.94-7.91 (d, 2H), 7.37-7.34 (m, 4H), 7.18-7.15 (m, 4H), 2.17-2.12 (m, 4H), 1.09-1.04 (m, 12H), 0.75-0.70 (m, 6H), 0.612 (m, 4H).

Synthesis of compound 2.1: To a 500mL round bottom flask, 0.750g (1.32mmol) boronate diester, 0.2430g (1.33mmol) 1,2-di-(4-pyridyl)ethylene, and 200mL benzene were added. The solution was allowed to reflux for 30 minutes then allowed to slowly cool to room temperature without disturbance upon which orange crystals grow on sides of flask. The solvent was decanted and the crystals were dried under vacuum for 30 minutes before collection of orange crystalline product (0.9172g, 76.8% yield). ^{1}H NMR (300 MHz, CD_2Cl_2): δ 8.68-8.66 (q, 4H), 7.94 (s, 2H), 7.92-7.89 (d, 2H), 7.84-7.82 (d, 2H), 7.51-7.49 (q, 4H), 7.29 (s, 2H), 7.22-7.19 (q, 4H), 7.04-7.01 (q, 4H), 2.11-2.05 (m, 4H), 1.09-1.02 (m, 12H), 0.75-0.70 (t, 6H), 0.59 (m, 4H).

Recrystallizations of supramolecular boronates general procedure: Recollected powder or crystals of the supramolecular boronate networks from previous experiments, with or without guest present, can be mixed together and recrystallized from desired solvent. This is done to recycle the material so that it can be reused instead of going to waste, and because it is faster and easier than synthesizing new material when more is needed. The general procedure is to add recollected powders to a round bottom flask along with the desired solvent (This works for several solvents not just benzene). The solution is allowed to reflux under N_2 atmosphere for 30 minutes to an hour before heating and stirring is stopped. Once reflux has stopped, a hot filtration into a clean round bottom flask is performed to remove any impurities that never dissolved, or precipitated out of solution after reflux stopped. The filtrate is then allowed to cool slowly along with slow evaporation to allow crystallization of desired supramolecular boronate network.

General procedure for solvent soaks and benzene reloading: To a 1 dram vial, 30-100mg of sample and 2mL of solvent are added. Vial is capped and allowed to sit for desired amount of time, usually 24 hours for normal benzene reloading. The sample is recollected via suction filtration using a side arm flask and hirsh filter funnel. The recollected sample is transferred from filter paper to a clean vial and dried under vacuum for 15 minutes.

Methods for determination of percent benzene: Three methods used for determination of percent benzene present **compound 2.1** are TGA, ^{1}H NMR, and simple mass by difference calculations. 1. TGA method: 10-30mg of sample are placed into an aluminum DSC pan and analyzed by the following method. Ramp 5°C/min to 150°C, Isothermal 5 minutes, Under He flow rate 100mL/min. 2. ^{1}H NMR method: Spectrum of sample is taken in CD_2Cl_2 and the peaks are integrated manually. The integration values are then used to determine the proton worth for the benzene and the proton worth for the protons on the network. A percent mass calculation is then performed based on the molecular formula of **compound 2.1** from the single crystal XRD data. The benzene proton worth is multiplied by 156.22 (the mass of 2 benzene molecules) and the network proton worth is multiplied by 908.77 (the mass of the network and 2 benzene molecules). A part over whole calculation is then performed to give the percent benzene. For accurate quantification of percent benzene by ^{1}H NMR non-standard NMR parameters must be used. I worked with Perry Pellechia to determine an accurate relaxation delay time for benzene by performing a T_1 experiment. After performing the study we have determined the proper parameters for accurate determination of percent benzene via ^{1}H NMR. A large relaxation delay (100 sec.) must be used or not all the benzene present

will actually be detected. Use of a relaxation delay of 100 seconds has allowed quantitative analysis of the percent benzene in the network via ^{1}H NMR. 3. Simple mass by difference calculations: This is used for removal on the large scale. Benzene is removed from the bulk sample by reduced pressure sublimation (kugelrohr) at 100°C for about an hour. The mass of the sample before and after removal of benzene are recorded and the numbers are used for a simple mass difference calculation to determine the percent of benzene that was present in the network.

Description of reloading methods used in reload method studies: Benzene was removed from **compound 2.1** by reduced pressure sublimation (kugelrohr) at 100°C for 1 hour prior to reloading. The four different reload methods are as follows: 1. undisturbed soak using the general procedure for solvent soaks described above. 2. Shaken soak using the general procedure for solvent soaks described above, but instead of letting sit undisturbed the vial is taped to an aliquot mixer in which the tray on the mixer continuously rocks back and forth. 3. Coffee filter with benzene stirring; the sample is placed in a coffee filter which is then clamped closed and hung into a glass sample tube containing 20mL of benzene. The coffee filter is completely submerged in the liquid benzene and a stir bar is at the bottom of the sample tube stirring the benzene. The sample tube is capped with a rubber septum. 4. Membrane tubing with benzene stirring. This method is the same as number 3 above, but instead of the sample being held in a coffee filter it is held in a molecular porous membrane tubing. Methods 1 and 2 are collected using filtration, while methods 3 and 4 are collected by transferring the sample from the membrane tube or coffee filter into a clean vial. All samples were dried under vacuum for 30 minutes in a lyophilizer container.

Procedure for BTEX mixture solvent study: Soaks in individual BTEX solvents were performed using the general procedure for solvent soaks described above. Three different BTEX mixtures were used, varying the ratio of benzene present in the mixture. An equal volume 1:1:1:1 mixture of benzene, toluene, ethylbenzene, and xylenes respectively was prepared as well as a 0.5:1:1:1 and 0.2:1:1:1 volumetric ratio mixtures. 35-60mg samples were used and the soaks were performed using the general procedure for solvent soaks, using 1 dram vials with 2mL of solution. These soaks were performed for 24 hours, 3 days, 3 days with agitation (using reloading method 2), and 7 days. All samples were isolated by filtration and dried under vacuum for 15 minutes.

2.10 References

[1] Rambo, B. M.; Lavigne, J. J. Defining Self-Assembling Linear Oligo(dioxaborole)s. *Chem. Mater*. **2007**, *19*, 3732-3739.

[2] Tilford, R. W.; Gemmil, W. R.; zur Loye, H.-C.; Lavigne, J. J. Facile Synthesis of a Highly Crystalline, Covalently Linked Porous Boronate Network. *Chem. Mater*. **2006**, *18*, 5296-5301.

[3] Sheepwash, E.; Krampl, V.; Scopelliti, R.; Sereda, O.; Neels, A.; Severin, K. Molecular Networks Based on Dative Boron-Nitrogen Bonds. *Angew. Chem. Int. Ed*. **2011**, *50*, 3034-3037.

[4] Christinat, N.; Croisier, E.; Scopelliti, R.; Cascella, M.; Rothlisberger, U.; Severin, K. Formation of Boronate Ester Polymers with Efficient Intrastrand Charge-Transfer Transitions by Three-Component Reactions. *Eur. J. Inorg. Chem*. **2007**, 5177-5181.

[5] Weijun, N.; Smith, M. D.; Lavigne, J. J. Self-Assembling Poly(dioxaborole)s as Blue-Emissive Materials. *J. Am. Chem. Soc*. **2006**, *128*, 16466-16467.

[6] Spek, A. L. Structure Validation in Chemical Crystallography. *Acta Cryst.* **2009**, *D65*, 148-155.

[7] Chadha, R.; Arora, P.; Saini, A.; Jain, D. S. Solvated Crystalline Forms of Nevirapine: Thermoanalytical and Spectroscopic Studies. *AAPS Pharm. Sci. Tech.* **2010**, *11*, 1328-1339.

[8] Goncalves, R. M. The Enthalpy and Entropy of Cavity Formation in Liquids and Corresponding States Principle. *Can. J. Chem*. **1990**, *68*, 1937-1949.

[9] Nishio, M. CH/π Hydrogen Bonds in Crystals. *Cryst. Eng. Comm.* **2004**, *6(27)*, 130-158.

[10] Sinnokrot, M. O.; Valeev, E. F.; Sherrill, C. D. Estimates of the Ab Initio Limit for π-π Interactions: The Benzene Dimer. *J. Am. Chem. Soc.* **2002**, *124*, 10887-10893.

[11] Larson, A. C.; Von Dreele, R. B. General Structure Analysis System (GSAS). *Los Alamos National Laboratory Report LAUR*. **1994**, 86-748.

[12] Toby, B. H. EXPGUI, a Graphical User Interface for GSAS. *J. Appl. Cryst*. **2001**, *34*, 210-213.

[13] PEDCo Environmental. *International Benzene Regulations.* PEDCo Environmental Inc. Cincinnati, Ohio, 1977.

Chapter 3 Toluene Inclusion Macrocycle and Hexagonal Phase

3.1 Overview

It has been previously shown that **compound 2.1** is selective towards adsorbing benzene and fluorobenzene while excluding other similar benzene derivatives. This prompted us to investigate how changing the solvent of crystallization while using the same building blocks as the SMB coordination polymer from benzene would affect the structure. Performing the same synthesis as shown in **Figure 2.2**, but varying the reaction solvent from benzene to toluene, afforded a new SMB macrocycle which contains the same building blocks but differs in the connectivity and guest inclusion. The formation of a SMB macrocycle is not unusual as boronic acids have been extensively employed in the construction of macrocycles and cages.[1]

What is more unusual is that changing the solvent of crystallization alone caused a significant change in structural connectivity, thus revealing that our system exhibits some type of solvent-induced polymorphism. Such observations imply that the free energy gaps between different crystal forms are small and the kinetic factors are most likely responsible for the crystal growth, and thus polymorphism is directed by crystallization conditions, such as solvent, reaction temperature and concentration effects.[2] Boronate ester formation, which is covalent yet reversible in nature, maintains all of the desired attributes of self-assembling materials including ease of synthesis and dynamic self-repair capability which allow the monomers to assemble into

thermodynamically favoured arrangement.[3] Such properties help attribute to the structural re-organization observed when the solvent of crystallization is changed.

Further investigation of related phenomena revealed that the polymorphic nature of this material is very unique and there are few examples of such systems in the literature. One related report used a polyol ring system exhibiting solvent dependent structural polymorphism in which a four-component boronate esters based macrocyclic ring system formed by the inclusion of a toluene molecule could be converted to a six-membered ring system upon replacement with two benzene molecules (**Figure 3.1**)[4].

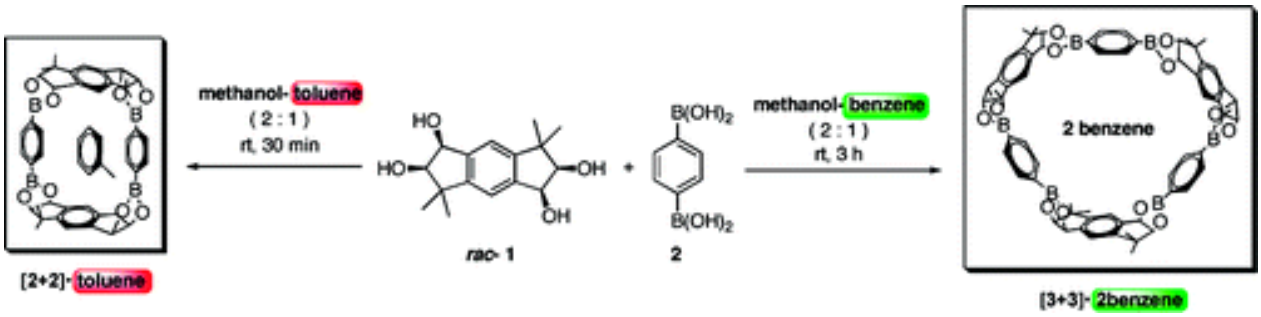

Figure 3.1: Synthetic scheme for a boronate ester based macrocyclic ring system formed from benzene diboronic acid and a racemic tetrol. The system exhibits solvent dependent structural polymorphism, forming a four-membered macrocycle with toluene inclusion upon synthesis in a 2:1 mixture of methonal:toluene and a six-membered macrocycle with benzene inclusion from synthesis in a 2:1 mixture of methanol:benzene.

Further studies of our SMB toluene inclusion macrocycle have revealed phenomena of co-crystallization of multiple phases as well as a single crystal to single crystal transformation. These properties could be promising for the development of useful applications such as molecular sensors or switches. More specifically we focused on the development of an optical sensor for benzene that can be observed by the naked eye. The discovery of a new hexagonal phase that co-crystallizes with **compound 3.1** exhibits promising properties for the ability to act as a benzene sensor.

3.2 SMB Macrocycle from Toluene, Compound 3.1

The Lavigne group has previously shown that using the same synthetic scheme as that of **compound 2.1** in **Figure 2.2**, but changing the solvent to toluene yields a SMB toluene inclusion compound with a macrocyclic structure (**compound 3.1**). Upon undisturbed slow cooling of the solution, dark red macrocycle crystals grew and were characterized by single crystal XRD.

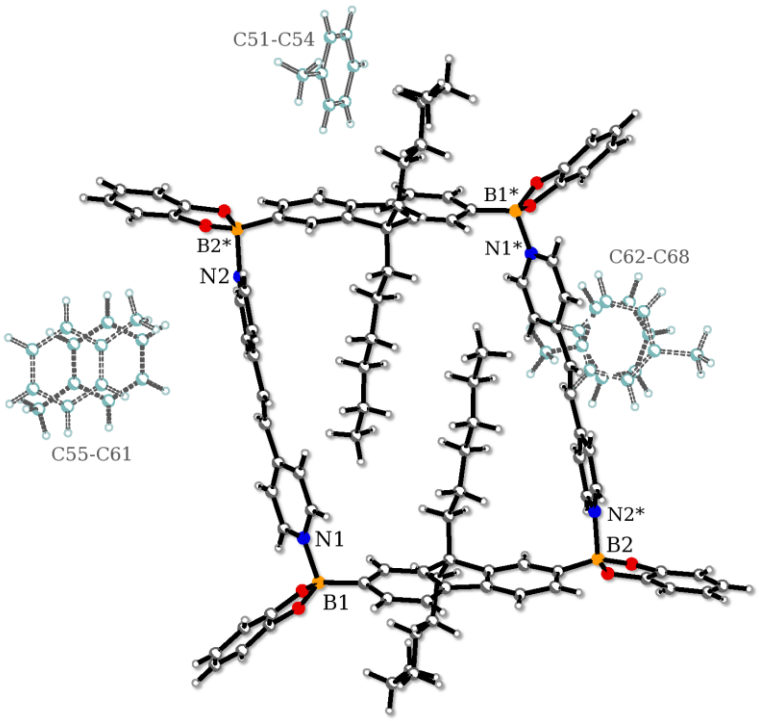

Compound 3.1

Figure 3.2: Unit cell of **compound 3.1** as determined by single crystal XRD. The compound crystallizes as macrocyclic units where two boronate diester backbones are linked together by two 1,2-dpe ligands. The disordered toluene guest molecules occupy void space between packing of macrocycle units.

Compound 3.1 crystallizes in the triclinic space group $P\bar{1}$ as confirmed by the successful solution and refinement of the structure from the single crystal XRD data. **Compound 3.1** has a unit cell of $[(C_{37}H_{40}B_2O_4)_2(C_{12}H_{10}N_2)_2]\cdot(C_7H_8)_{3.62}$ which consists of

macrocycle units with toluene molecules filling the void space as shown in **Figure 3.2**. The theoretical amount of toluene retained by **compound 3.1** represents 18.1% of the total mass of the network. ^{1}H NMR analysis confirmed the presence of toluene and TGA was used to determine an experimental 18.1% mass loss of toluene (**Figure 3.3**).

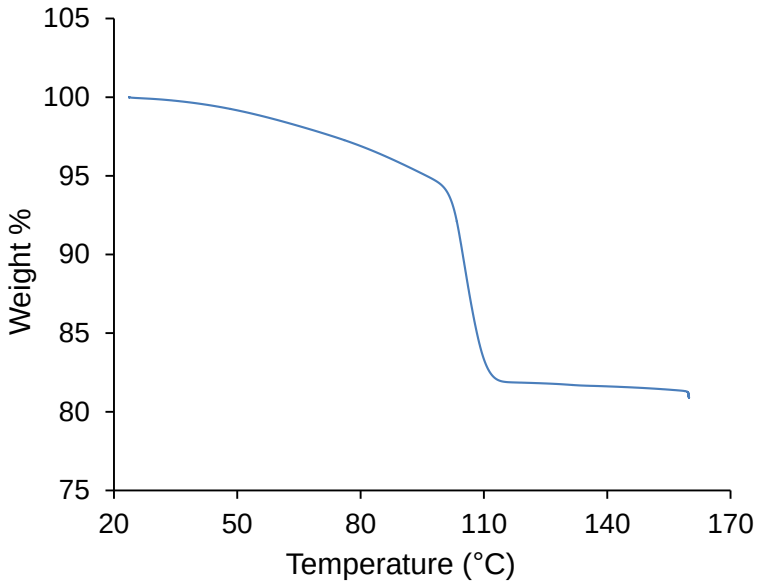

Figure 3.3: TGA plot of crystals of **compound 3.1** showing the weight % loss of toluene from the network which occurs around the 110°C boiling point of toluene.

Loss of toluene from **compound 3.1** is accompanied with a color change from red to yellow as seen in **Figure 3.4**. After removal of toluene via TGA desolvated **compound 3.1** was soaked in liquid toluene to see if the macrocycle would re-adsorb its guest like **compound 2.1** was seen to do. After a 43 hour liquid toluene soak the material remained yellow and no toluene was re-adsorbed as evidenced by ^{1}H NMR and TGA.

The same sample of desolvated **compound 3.1** was then immersed in liquid benzene overnight resulting in the adsorption of benzene. Further studies showed that if **compound 3.1** was soaked in liquid benzene, the toluene is replaced by benzene

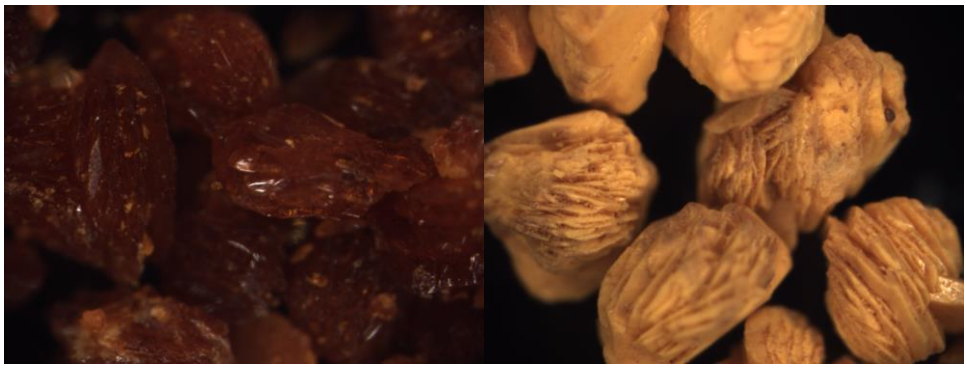

Figure 3.4: Optical microscope pictures of initial solvated crystals of **compound 3.1** (left) and desolvated **compound 3.1** (right). After toluene removal a distinct color change from dark red to pale yellow is observed.

accompanied by a structural transformation from **compound 3.1** to **compound 2.1** as confirmed by ^{1}H NMR and PXRD (**Figure 3.5**). This unique structural transformation prompted us to investigate if a similar transformation occurs when **compound 3.1** is exposed to benzene vapors.

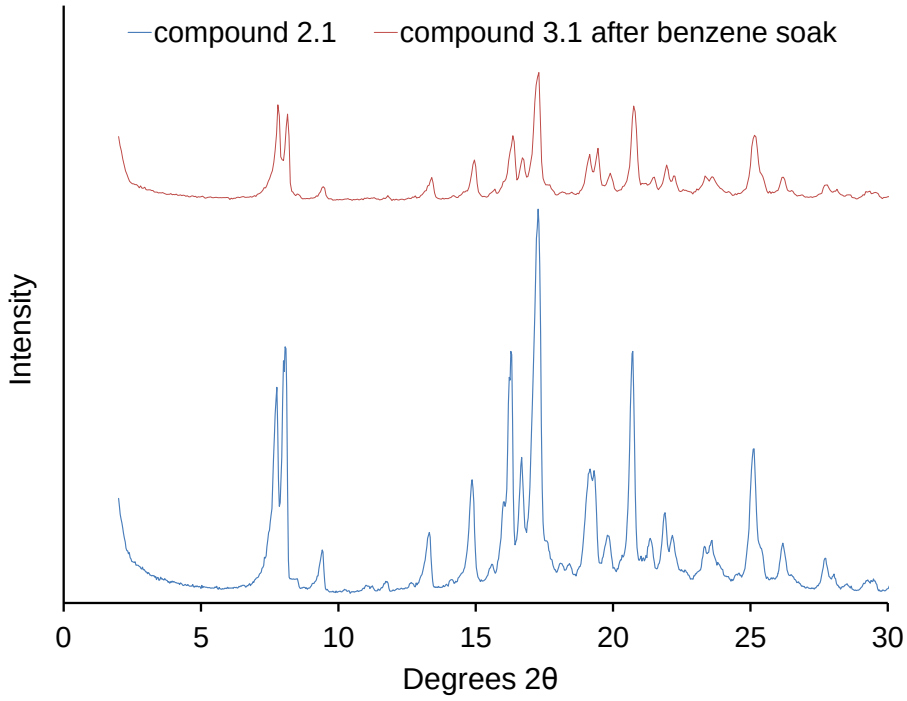

Figure 3.5: PXRD of **compound 3.1** after being soaked in liquid benzene (red) and PXRD of crystals of **compound 2.1** (blue). The matching PXRD patterns confirm that upon immersion in liquid benzene, **compound 3.1** converts to **compound 2.1**.

Preliminary studies had shown that upon exposure to benzene vapors in a closed chamber, the toluene in **compound 3.1** was exchanged with benzene while maintaining the macrocyclic single crystal quality, and that this exchange was accompanied by a color change from red to yellow.[5] Upon reinvestigation of this single crystal transformation, single crystal XRD of **compound 3.1** before and after the benzene vapor soak confirmed the exchange of benzene for toluene without loss of single crystallinity, but optical microscope images of the macrocycle crystals before and after the benzene vapor soak showed no associated color change (**Figure 3.6**). The crystal after the exchange experiment retained good crystallinity, and all the toluene has been replaced with benzene. The benzenes are in roughly the same positions as the toluene molecules were, but the exchange compound appears to be stoichiometric, with 4 benzenes per macrocycle verse the 3.62 toluenes per macrocycle in the initial crystals.

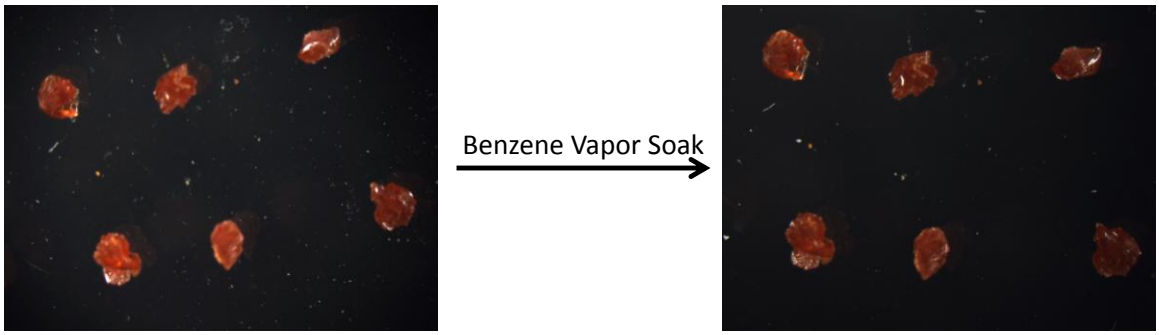

Figure 3.6: Optical microscope pictures of macrocycle crystals of **compound 3.1** before (left) and after (right) exchange of toluene with benzene achieved during a benzene vapor soak. The solvent exchange occurred without loss of single crystallinity.

3.3 Hexagonal Phase Co-Crystallization with Compound 3.1

Recently we have discovered a new structure (**compound 3.2**) in this class from toluene that is not a macrocycle, but instead a zigzag 1-D polymeric chain that packs in a hexagonal fashion with the inclusion of toluene guest molecules (**Figure 3.7**). We have

obtained single crystal XRD data on this phase, but further refinement to determine the unit cell lattice parameters is still needed.

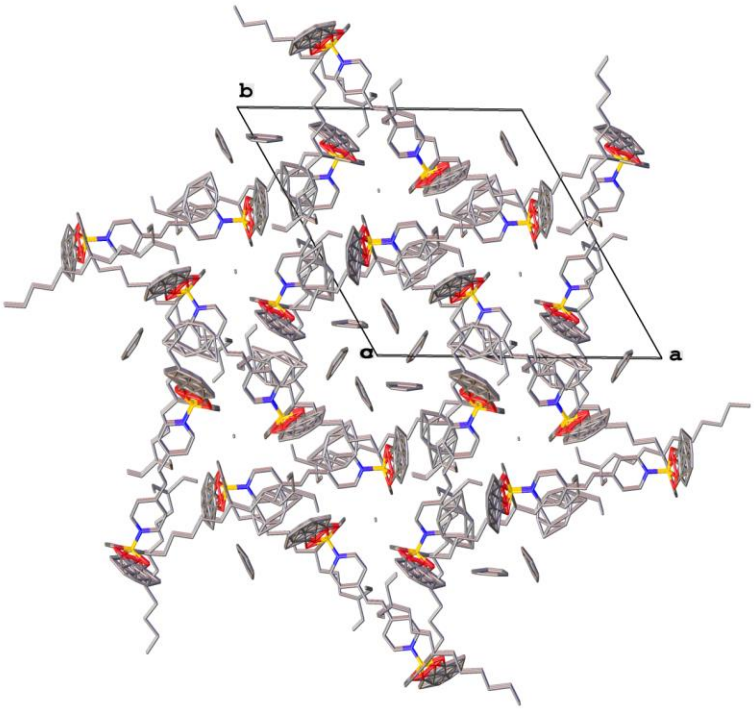

Figure 3.7: Hexagonal fashion packing of 1-D polymeric chains of **compound 3.2**. Toluene guest molecules occupy the void space between the packing of the chains. This figure was generated from preliminary refinement of the single crystal XRD data and disorder in the boronate ester backbones is clearly seen.

Crystals of **compound 3.2** were discovered during an attempt to synthesize and crystallize **compound 3.1**, upon which a block of large yellow sheet crystals appeared during crystallization instead of the expected dark red macrocycle crystals of **compound 3.1**. These crystals were taken to our staff crystallographer, but due to poor diffraction quality only preliminary results were obtained. Our crystallographer reported that theses crystals diffract quite poorly, with very strong reflections at low angle, but nothing at

higher scattering angles because of extensive disorder in the crystal. He also reported that these crystals desolvate and lose all diffracting power in a few hours if kept in air.

Further attempts to selectively crystallize the hexagonal **compound 3.2** over the macrocyclic **compound 3.1** from toluene proved unsuccessful as **compound 3.2** was only seen to co-crystallize with **compound 3.1**. It is fairly easy to identify this co-crystallization because crystals of **compound 3.2** are faint yellow, whereas the crystals of **compound 3.1** are dark red in solution. At first, **compound 3.2** was identified due to the large yellow block crystals that appeared during crystal growth, but further attempts of crystallization showed that small yellow crystals of **compound 3.2** can also grow along with the red macrocycle crystals of **compound 3.1** as shown in **Figure 3.8**. Attempts were made to separate the two phases during isolation, but this proved very difficult because the yellow hexagonal crystals of **compound 3.2** change color from light yellow to dark orange upon removal from toluene. After isolation of the crystals both phases are dark orange red in color, making it difficult to tell the difference between the phases.

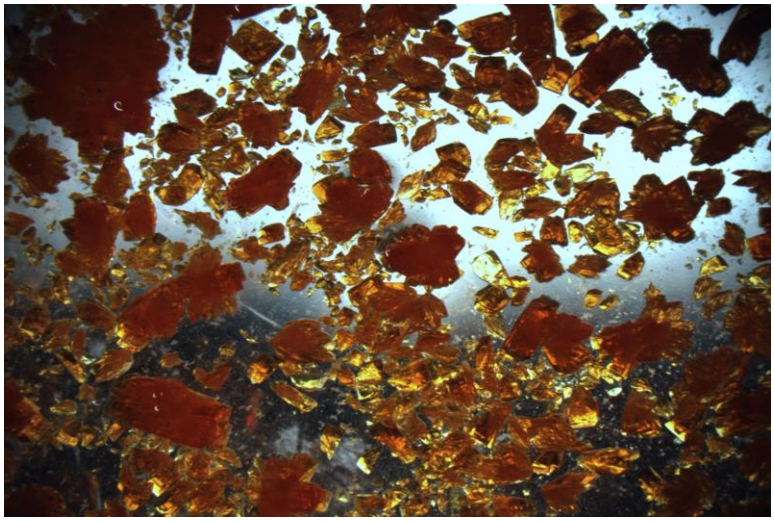

Figure 3.8: Optical microscope image of co-crystallization of **compound 3.2** with **compound 3.1**. **Compound 3.1** are the larger dark red block-like crystals whereas **Compound 3.2** are the smaller yellow crystals.

Another phenomenon that was observed with the two phase co-crystallization was that over time the yellow hexagonal phase crystals of **compound 3.2** seem to convert to the dark red macrocycle crystals of **compound 3.1**. This was confirmed by our staff crystallographer who, due to a high volume of samples, had to allow the flask containing crystals of **compound 3.2** to sit for about two weeks before he was able to analyze them. When he went to analyze the crystals, only red macrocycle crystals of **compound 3.1** were present in the flask, thus confirming that over time crystals of **compound 3.2** convert to crystals of **compound 3.1**. Such a phenomenon tells us that the red macrocycle crystals of **compound 3.1** may be the more thermodynamically stable product; while the yellow hexagonal crystals of **compound 3.2** may be the kinetically favored product as they usually grow first when this co-crystallization is observed. Further crystallization experiments need to be performed to better understand the relationship between the two polymorphs and their dependence on thermodynamics and kinetics.

It is unknown what dictates the formation of macrocyclic **compound 3.1** versus the hexagonal **compound 3.2** in toluene, and further studies are needed to determine the adsorption and associated optical properties of the newly discover **compound 3.2**. The molecular arrangement in crystals frequently decides the functionality and properties and thus one polymorph may exhibit unwanted properties while the other exhibits the desired properties, making the precise control of crystallization of polymorphs a very important topic.[6] Controlling the crystallization of one polymorph over the other is a difficult task, and one must have a strong understanding of crystal engineering and the ability to control thermodynamic and kinetic factors of nucleation and growth. The selective

crystallization of a polymorph depends not only on the initial nucleation, but also on cross-nucleation and relative growth rates of the polymorphs.[7] Although it is possible to selectively crystallize one polymorph over another, it is a difficult task and we have been unable to discover a crystal growth procedure to selectively yield **compound 3.2** over **compound 3.1**.

3.4 Compound 3.2 as a Benzene Sensor

Some preliminary experiments utilizing the newly discovered **compound 3.2** have shown very promising adsorption and optical properties that could result in a benzene sensor that can be detected by the naked eye. There are several currently accepted methods for benzene monitoring and analysis, the most common being GC-MS, which uses expensive equipment that is not readily portable for field analysis. More recently, the implementation of optical sensors applicable for field measurements of BTEX have been created.[8] These optical sensors are based on fiber optics coated with a special polymer in which BTEX is predominantly adsorbed causing a change in the optical properties that can be used to determine concentrations of the BTEX components adsorbed.[9] This sensor exhibits good sensitivity, but is not specific towards benzene, the most toxic of the BTEX class. None of the current methods can be used for naked eye detection of benzene which would allow for the development of a benzene warning badge similar to that of the radiation badge. The discovery of materials that can sense benzene in a reversible, selective, yet cost effective method is of great interest for such applications and thus there is room for improvement in current benzene detection methods.

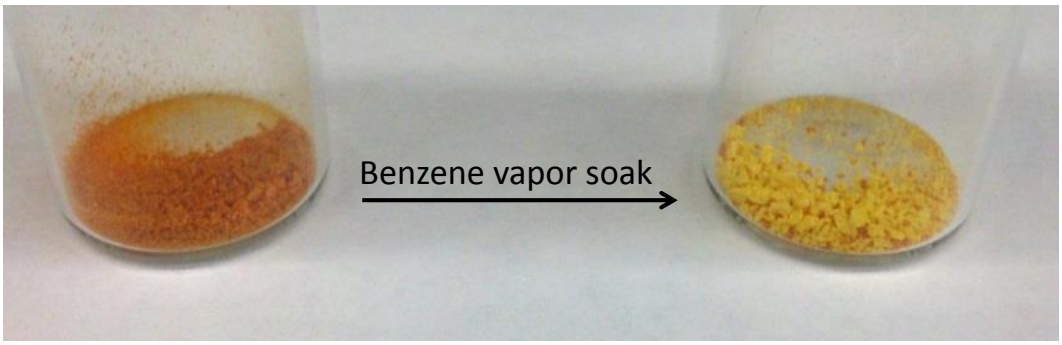

Figure 3.9: Image of the observed color change from dark orange to yellow that **compound 3.2** undergoes upon exposure to benzene vapors. If you look closely at the vial on the right you can see specs of red which are **compound 3.1** that co-crystallizes with **compound 3.2** and complete separation of the two polymorphs is very difficult.

Compound 3.2 has shown the ability to act as a benzene sensor based on some preliminary experimentation. As previously stated, **compound 3.2** appears as dark red orange hexagonal crystals that look very similar to **compound 3.1** when isolated from toluene. When crystals of **compound 3.2** are exposed to benzene vapors a distinct color change from dark orange to yellow is observed (**Figure 3.9**). I have confirmed through ^{1}H NMR that the guest toluene molecules are replaced by benzene guest molecules.

The distinct color change upon exposure to benzene vapors is a unique property that we would like to utilize for benzene sensing applications, but further research on **compound 3.2** needs to be performed to determine the feasibility of using the material as a benzene sensor. The idea is that this naked eye sensor would be a cost effective way of indicating if dangerous levels of benzene are present. Such could be compared to a smoke detector or carbon monoxide detector, alerting people of a hazard without the need for the expensive, time consuming methods used to measure specific concentration present.

3.5 Conclusion

In conclusion, we have discovered that our SMB system exhibits fairly unique properties of polymorphism and co-crystallization. Using the same building blocks, but changing the solvent of crystallization causes a complete change in the structural connectivity of the network from 1-D polymeric zigzag chains to macrocyclic units. This shows that our SMB system exhibits solvent dependent polymorphism. Not only do we see solvent dependent polymorphism, but we also see co-crystallization of two phases or polymorphs from toluene. The new phase (**compound 3.2**) from toluene was found to be composed of 1-D polymeric zigzag chains packed in a hexagonal fashion, unlike any other SMB coordination polymer observed in our system. **Compound 3.2** has been observed to undergo a distinct color change from dark orange to yellow upon exposure to benzene vapors, a property that could potentially be utilized for optical benzene sensing applications. Future work needs to be dedicated to understanding the thermodynamic and kinetics of the co-crystallization in toluene with an end goal of being able to control preferential crystal growth of one phase over the other. The ability to selectively isolate **compound 3.2** over **compound 3.1** needs to be achieved to enable further studies of the optical and adsorption properties for utilization in benzene sensing applications.

3.6 Experimental

Synthesis of toluene inclusion macrocycle (compound 3.1): To a 250mL round bottom flask, 0.5028g (0.882mmol) boronate diester, 0.1853g (1.02mmol) 1,2-di-(4-pyridyl)ethylene, and 50mL toluene were added. The solution was heated to reflux and after 15 minutes was allowed to slowly cool to room tempreature without disturbance. Dark red crystal were obtained after 10 days of slow evaporation. The solvent was

decanted and the crystals were dried under vacuum for 30 minutes (0.6156g, 37.9% yield). ^{1}H NMR (300 MHz, CD_2Cl_2): δ 8.69-8.67 (q, 4H), 7.91 (s, 2H), 7.88-7.85 (d, 2H), 7.82-7.79 (d, 2H), 7.52-7.50 (q, 4H), 7.26 (s, 2H), 7.18-7.16 (q, 4H), 7.01-6.98 (q, 4H), 2.10-2.04 (m, 4H), 1.11-1.01 (m, 12H), 0.75-0.70 (t, 6H), 0.59 (m, 4H).

Synthesis of toluene hexagonal phase (compound 3.2): Synthesis is the same as the **compound 3.1** above. It is important to note that this phase sometimes co-crystallizes with the toluene inclusion macrocycle and we have yet to synthesis this hexagonal phase alone, therefore there is no specific synthetic route or yield to report. The yellow sheet crystals grow after 1-2 weeks of undisturbed slow evaporation. ^{1}H NMR (300 MHz, CD_2Cl_2): δ 8.69-8.67 (q, 4H), 7.91 (s, 2H), 7.88-7.85 (d, 2H), 7.82-7.79 (d, 2H), 7.52-7.50 (q, 4H), 7.26 (s, 2H), 7.18-7.16 (q, 4H), 7.01-6.98 (q, 4H), 2.10-2.04 (m, 4H), 1.11-1.01 (m, 12H), 0.75-0.70 (t, 6H), 0.59 (m, 4H). It is also important to note the the ^{1}H NMR data is identical to **compound 3.1** because the components of the network are identical and only the connectivity and packing are different.

General procedure for solvent soaks: To a 1 dram vial, 30-100mg of sample and 2mL of solvent are added. Vial is capped and allowed to sit for desired amount of time. The sample is recollected via suction filtration using a side arm flask and hirsh filter funnel. The recollected sample is transferred from filter paper to a clean vial and dried under vacuum for 15 minutes.

General procedure for vapor soaks: To a 10mL beaker, 30-150mg of sample are added. The beaker is then placed in a TLC chamber to which about 50mL of desired solvent is added. The chamber is closed and allowed to sit undisturbed for desired

amount of time. After the soak the beaker is removed from the chamber and the sample is transferred to a clean vial and dried under vacuum for 15 minutes.

Methods for determination of percent toluene: The methods for determination of percent toluene in the macrocycle are the same as those for **compound 2.1** which are described in detail in the experimental section of **Chapter 2**.

3.7 References

[1] Christinat, N.; Scopelliti, R.; Severin, K. Multicomponent Assembly of Boronic Acid Based Macrocycles and Cages. *Angew. Chem. Int. Ed.* **2008**, *47*, 1848-1852.

[2] Peng, R.; Deng, S-R.; Li, M.; Li, D.; Li, Z-Y. Solvent-Dependent Copper(I) Conformational Supramolecular Pseudo-Polymorphs Based on a Flexible Thioether Ligand. *Cryst. Eng. Comm.* **2008**, *10*, 590-597.

[3] Tilford, R. W.; Mugavero, S. J.; Pellechia, P. J.; Lavigne, J. J. Tailoring Microporosity in Covalent Organic Frameworks (COFs). *Adv. Mater*. **2008**, *20*, 2741-2746.

[4] Iwasawa, N.; Takahagi, H. *J. Am. Chem. Soc.* **2007,** *129*, 7754-7755.

[5] Sapp, K. M.S. Dissertation, University of South Carolina, 2011.

[6] Kitamura, M. Strategy for Control of Crystallization of Polymorphs. *Cryst. Eng. Comm.* **2009**, *11*, 949-964.

[7] Yu, L. Survival of the Fittest Polymorph: How Fast Nucleater Can Lose to Fast Grower. *Cryst. Eng. Comm.* **2007**, *9*, 847-851.

[8] Drew, S.; Smith, L.; McGee, K.; Mann, K. *Chem. Mater.* **2009,** *21*, 3117-3124.

[9] Veen, J.; Saini, D.; Hal, R.; Heimovaara, T. *Development of an optical sensor for BTEX and chlorinated ethylenes.* NOBIS-project:97-1-09.

Chapter 4 SMB Coordination Polymer Analogues and Solvent Induced Polymorphs

4.1 Overview

Discovering new materials with unique and applicable properties has and will continue to be of great interest and boronic acid based materials have seen a significant increase in applications of self-assembly, sensing and separations.[1] The reversibility of boronate esters and B-N dative bonds has allowed for the discovery of several new crystalline SMB coordination polymers and macrocycles. I have previously shown that changing the solvent of crystallization from benzene to toluene while leaving our SMB building blocks unchanged results in solvent induced polymorphism from a benzene inclusion coordination polymer consisting of 1-D polymeric zigzag chains (**compound 2.1**) to a toluene inclusion macrocycle (**compound 3.1**). These results, along with the selective adsorption of benzene and fluorobenzene by **compound 2.1** prompted us to use other benzene derivatives as solvents of crystallization in our SMB system. Performing the same synthesis as shown in **Figure 2.2**, but varying the reaction solvent from benzene to other benzene derivatives afforded several new SMB networks, all which contain the same building blocks but differ in their connectivity and or guest inclusion.

We have also taken a reticular synthesis approach to discover new SMB materials by altering the starting building blocks.[2,3,4] Adding electron donating or withdrawing groups as substituents to the catechol portion may alter the electronic properties of the system and induce optical transitions which may lead intense color changes upon guest

adsorption and desorption.[5] We can also alter the diamine linker, changing the size and shape, which will ultimately change the pore size and possibly the shape of the networks. It is expected that such changes could lead to different guest adsorption and selectivity properties.

4.2 Macrocycle from Xylenes, Compound 4.1

Performing the same general synthesis shown in **Figure 2.2** with 9,9-dihexylfluorene-2,7-diboronic acid, catechol, and 1,2-dpe, but using xylenes as the reaction solvent yields a SMB macrocycle with xylene guest inclusion (**compound 4.1**). The small dark orange block crystals were obtained through slow evaporation of the transparent yellow solution over a three week period. The structure is essentially the same as **compound 3.1** discussed in **Chapter 3**, except for the difference in the guest molecules present. Single crystal XRD analysis confirmed that **compound 4.1** crystallizes in the triclinic space group $P\bar{1}$. The asymmetric unit consists of half of one $[(C_{37}H_{40}B_2O_4)_2(C_{12}H_{10}N_2)_2]$ macrocycle, which is located on a crystallographic inversion center, and three independent volumes of disordered xylene solvent species as seen in **Figure 4.1**. This yields an overall molecular formula of $[(C_{37}H_{40}B_2O_4)_2(C_{12}H_{10}N_2)_2]\cdot 3.78(C_8H_{10})$ which corresponds to a theoretical % mass of 21.1% xylenes. Analysis for experimental % mass of xylenes was performed by TGA which showed an 18.2% mass loss due to xylenes and ^{1}H NMR was performed as further structural confirmation.

The xylenes are badly disordered as can be seen from **Figure 4.1**, and the model worked out for structural solution has all the species as meta-xylene. Para-xylene was unable to fit in the structure, but ortho-xylene is a possibility although it was omitted

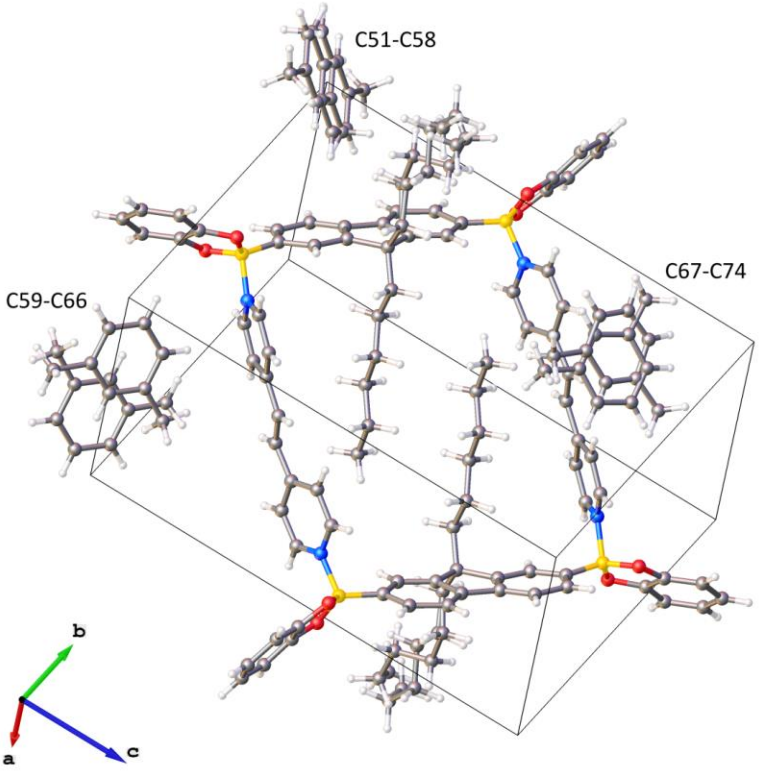

Compound 4.1

Figure 4.1: Unit cell of **compound 4.1** as determined by single crystal XRD. The compound crystallizes as macrocyclic units where two boronate diester backbones are linked together by two 1,2-dpe ligands in an identical fashion to **compound 3.1**. The disordered xylene guest molecules occupy void space between packing of macrocycle units.

from the final structural solution. It should be stressed that there is high uncertainty in the solvent content because of the disorder and therefore it should not be claimed that these crystals show 100% selectivity for including meta-xylene. There is probably some ortho-xylene included in the compound, but it cannot be seen conclusively based on the XRD data. It should be noted that this is a fairly common issue when using xylenes as a crystallization solvent because they frequently end up in the crystal as disordered mixtures which are difficult to sort out.[6]

In an attempt to re-synthesize **compound 4.1**, the slow evaporation crystal growth afforded large yellow crystals which resemble the hexagonal **compound 3.2** that was found to co-crystallize with **compound 3.1** as discussed in **Section 3.3**. These crystals were taken to our staff crystallographer who reported that since submission of these crystals, many large clusters of red-orange crystals have been appearing in the flask in addition to the large yellow crystals already present. He was able to confirm the clusters of red-orange crystals as **compound 4.1**, while the yellow crystals he confirmed as the large hexagonal phase shown in **Figure 3.6** with the inclusion of xylenes instead of toluene. He reported that over time the large yellow hexagonal phase crystals all slowly converted to red macrocycle crystals of **compound 4.1**. As discussed in **Section 3.3**, no full structural solution of the large hexagonal phase has yet to be obtained, but its appearance co-crystallizing with **compound 4.1** suggests that this phase is not specific to crystallizing in just toluene, but may appear in several other solvents as well.

4.3 Macrocycle from Styrene, Compound 4.2

Performing the same general synthesis shown in **Figure 2.2** with 9,9-dihexylfluorene-2,7-diboronic acid, catechol, and 1,2-dpe, but using styrene as the reaction solvent yields a SMB macrocycle with styrene guest inclusion (**compound 4.2**). The orange block-like crystals were obtained through slow evaporation of the transparent solution over a 1-2 week period. Single crystal XRD analysis confirmed that **compound 4.2** crystallizes in the triclinic space group $P\bar{1}$. The asymmetric unit consists of half of one $[(C_{37}H_{40}B_2O_4)_2(C_{12}H_{10}N_2)_2]$ macrocycle complex located on a crystallographic inversion center, and three independent regions containing styrene molecules as seen in **Figure 4.2**.

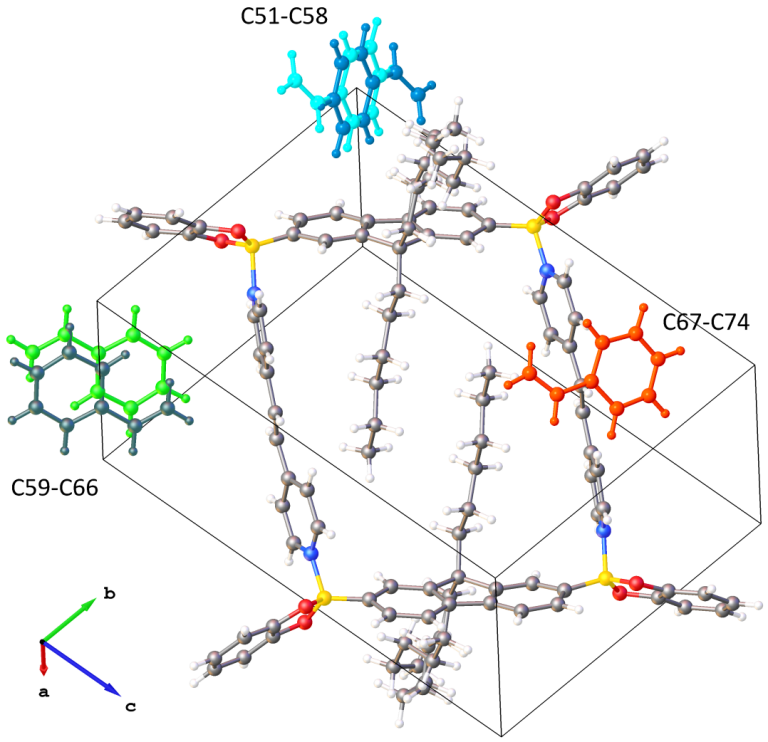

Compound 4.2

Figure 4.2: Unit cell of **compound 4.2** as determined by single crystal XRD. The compound crystallizes as macrocyclic units where two boronate diester backbones are linked together by two 1,2-dpe ligands in an identical fashion to **compounds 3.1** and 4.1. The disordered styrene guest molecules occupy void space between packing of macrocycle units.

Compound 4.2 has the same basic structure as **compound 3.1**, except that styrene has replaced toluene in the crystal. The unit cell parameters are similar, and the crystal packing is essentially the same. The styrene molecules occupy the same interstitial sites as the toluene molecules did, but in this case they fully occupy their sites, resulting in 4 styrene molecules per macrocycle, versus 3.62 toluene molecules in **compound 3.1**. This yields an overall molecular formula of $[(C_{37}H_{40}B_2O_4)_2(C_{12}H_{10}N_2)_2]\cdot 4(C_8H_8)$ which corresponds to a theoretical % mass of 21.7% styrene. Analysis for experimental % mass of styrene was performed by TGA and ^{1}H

NMR which gave results of 21.3% and 20.8% respectively. No further experiments were performed with these crystals, but it would be interesting to investigate adsorption properties such as selectivity, exchange and the possible associated optical properties.

4.4 Modified Toluene Macrocycle, Compound 4.3

Following the same synthetic scheme used to obtain **compound 3.1**, but changing two of the three building blocks afforded a new SMB toluene inclusion macrocycle (**compound 4.3**). The boronate diester motif was formed using the same diboronic acid (9,9-dihexylfluorene-2,7-diboronic acid), but using 3-methoxycatechol as the 1,2-diol linkage as shown in **Figure 4.3**.

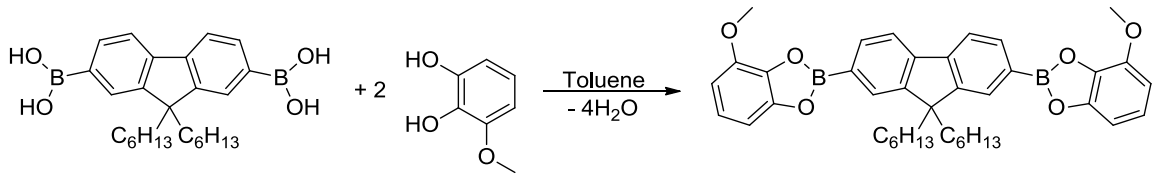

Figure 4.3: Synthetic scheme showing the condensation reaction between 9,9-dihexylfluorene-2,7-diboronic acid and 3-methoxycatechol to yield the 3-methoxycatechol substituted boronate diester used in the synthesis of **compound 4.3**.

The boronate diester containing methoxy substituents was then reacted with 1,3-di-(4-pyridyl)propane as the diamine linker. Undisturbed slow evaporation of the colorless solution resulted in colorless plate crystals of **compound 4.3**. Single crystal XRD analysis confirmed that **compound 4.3** crystallizes in the triclinic space group $P\ \bar{1}$ as determined by structural solution. The asymmetric unit consists of half of one $[(C_{39}H_{44}B_2O_5)_2(C_{13}H_{14}N_2)_2]$ macrocycle molecule located on a crystallographic inversion center, and two toluene molecules of crystallization which gives 4 toluene molecules per macrocycle (**Figure 4.4**).

It is important to note that there is some crystallographic disorder of one entire -$BO_2C_6H_3OCH_3$ group and part of a hexyl substituent. The -$BO_2C_6H_3OCH_3$ group adopts

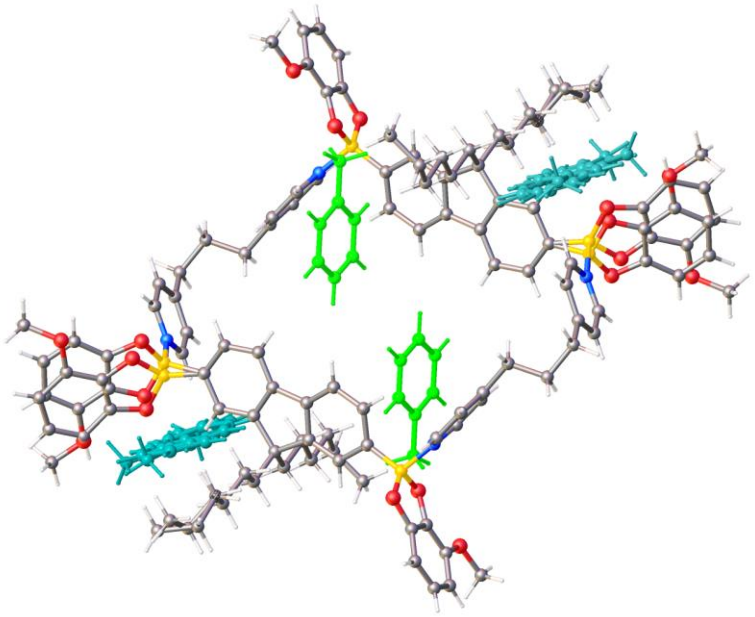

Compound 4.3

Figure 4.4: Unit cell of **compound 4.3** as determined by single crystal XRD. The compound crystallizes as macrocyclic units where two, 3-methoxycatechol containing boronate diester backbones are linked together by two 1,3-di-(4-pyridyl)propane ligands. The toluene guest molecules occupy void space between packing of macrocycle units.

two orientations throughout the crystal as can be seen in **Figure 4.4**. It is interesting to note that even though the diamine linker is different than the one used for the macrocyclic **compounds 3.1**, **4.1** and **4.2** previously reported, **compound 4.3** still crystallizes in the same space group. **Compound 4.3** has an overall molecular formula of $[(C_{39}H_{44}B_2O_5)_2(C_{13}H_{14}N_2)_2]\cdot 4(C_7H_8)$ which constitutes a theoretical % mass of 18.2% toluene. Unfortunately, no further data or preliminary results on **compound 4.3** have been collected due to loss of the sample and difficulty in re-obtaining crystal.

4.5 Fluorobenzene SMB Coordination Polymer, Compound 4.4

Solvent adsorption studies performed using **compound 2.1** showed that fluorobenzene was adsorbed by the desolvated form. Based on those results, I

hypothesized that recrystallization from fluorobenzene would yield an identical SMB coordination polymer as **compound 2.1**, except for a difference in the guest inclusion. A sample of desolvated **compound 2.1** was dissolved in hot fluorobenzene affording a transparent gold solution. The solution was removed from heat and allowed to cool slowly without disturbance resulting in the growth of orange clusters of crystals of **compound 4.4** overnight. The single crystal removed from a cluster of crystals was reported as a yellow almond-shaped plate crystal. Single crystal XRD analysis confirmed that **compound 4.4** crystallizes in the monoclinic space group $P2_1/n$ which is the same as **compound 2.1**. The asymmetric unit consists of one $[(C_{37}H_{40}B_2O_4)(C_{12}H_{10}N_2)]$ polymeric complex, half each of two fluorobenzene molecules located on inversion centers, and another complete fluorobenzene molecule as seen in **Figure 4.5**.

Compound 4.4 is essentially identical to **compound 2.1** discussed in **Chapter 2**, except that the benzene molecules have been replaced by fluorobenzene, giving the compound a molecular formula of $[(C_{37}H_{40}B_2O_4)(C_{12}H_{10}N_2)]\cdot 2C_6H_5F$. It is interesting to note that based on the distribution of disordered C_6H_5F molecules, it looks like meta-, para-, or ortho- difluorobenzene could fit into the structure and even possibly 1,2,4,5-tetrafluorobenzene. No experiments were conducted to test if this SMB coordination polymer would adsorb either difluorobenzene or tetrafluorobenzene.

Some preliminary results were obtained for **compound 4.4** such as, % fluorobenzene by TGA and ^{1}H NMR, desorption/re-adsorption of the guest, and selectivity test towards benzene verse fluorobenzene. TGA showed a 21.9% mass loss of fluorobenzene and was further confirmed by ^{1}H NMR which gave a calculated value of 21.9% fluorobenzene. These values compare fairly well with the theoretical 20.4% mass

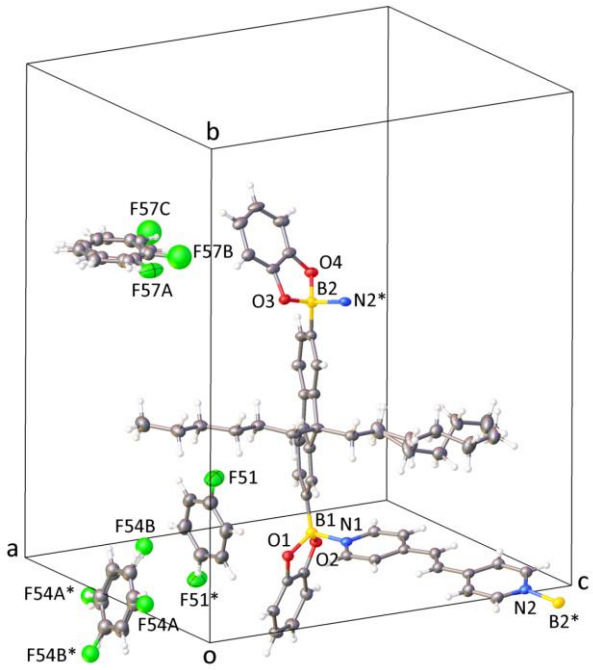

Compound 4.4

Figure 4.5: Unit cell of **compound 4.4** as determined by single crystal XRD. The compound crystallizes as 1-D polymeric zigzag chains identical to those of **compound 2.1**. The only difference between this compound and **compound 2.1** is that the void space between the packing of the 1-D polymeric chains is occupied by disordered fluorobenzene guest molecules instead of benzene.

of fluorobenzene. After removal of the fluorobenzene guest by TGA, desolvated **compound 4.4** was soaked in liquid fluorobenzene for 26 hours to evaluate the ability to re-adsorb its guest. TGA and ^{1}H NMR both confirmed that fluorobenzene was re-adsorbed by the network giving values of 21.8% and 19.9% fluorobenzene respectively. To test if benzene would replace fluorobenzene, the initial crystals of **compound 4.4** were soaked in liquid benzene for 23 hours. It can be clearly seen from the ^{1}H NMR that benzene does not replace the fluorobenzene as evidence by the absence of the sharp

singlet benzene peak at 7.35ppm, while the fluorobenzene peaks remain present (**Figure 4.6**).

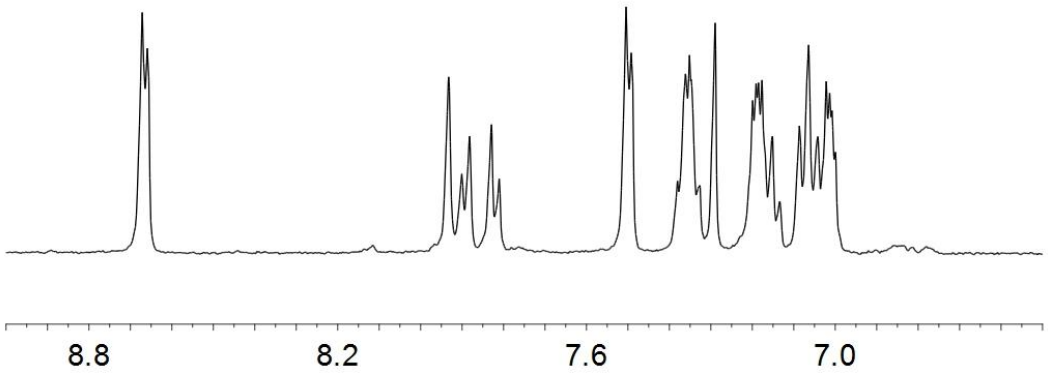

Figure 4.6: ^{1}H NMR spectrum of **compound 4.4** after immersion in liquid benzene for 23 hours. It is clear that benzene was not absorbed evidenced by the absence of a shape singlet at 7.35ppm representative of benzene. Instead we see a combination of two doublets that are representative of fluorobenzene.

This experiment was also performed in the vapor phase upon which initial crystals of **compound 4.4** were exposed to benzene vapors in a sealed container for 9 days. Once again the fluorobenzene was not exchanged by benzene as evidenced by ^{1}H NMR. These results seem to suggest that the SMB coordination polymer has a stronger affinity for fluorobenzene then it does for benzene. Further studies could be performed to evaluate the enthalpy of desolvation of fluorobenzene from **compound 4.4** and compare it to the value obtained for benzene as reported in **Section 2.3**. It would also be interesting to see if immersion of **compound 2.1** in fluorobenzene would result in solvent exchange.

4.6 Chlorobenzene SMB Coordination Polymer, Compound 4.5

Previous attempts to adsorb chlorobenzene with desolvated **compound 2.1** proved inconclusive. I hypothesized that if chlorobenzene was able to fit into the pores of the SMB coordination polymer, than recrystallization in chlorobenzene would yield an identical compound to **compound 2.1**, but with different guest molecules as was

observed with **compound 4.4**. A sample of desolvated **compound 2.1** was dissolved in hot chlorobenzene, resulting in a transparent gold solution which was then allowed to cool slowly without disturbance. Slow evaporation over a one month period resulted in a few orange clusters of crystals of **compound 4.5**. The single crystal removed from a cluster of crystals was reported as a yellow plate-like crystal. Single crystal XRD analysis confirmed that **compound 4.5** crystallizes in the monoclinic space group $P2_1/n$ with the asymmetric unit consisting of one $[(C_{37}H_{40}B_2O_4)(C_{12}H_{10}N_2)]$ polymeric complex and three chlorobenzene molecules as shown in **Figure 4.7**.

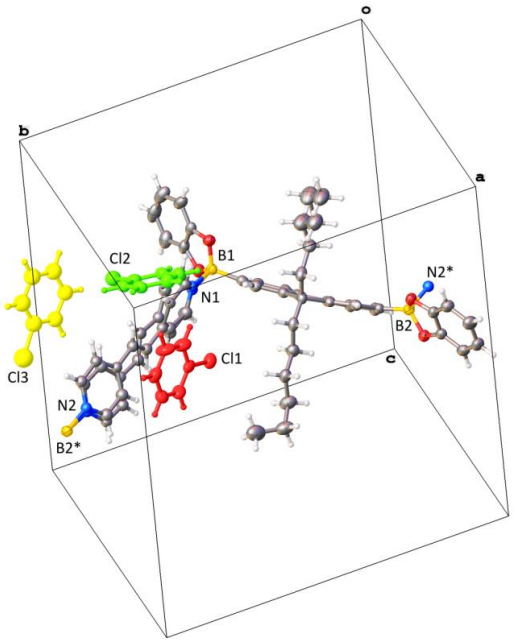

Compound 4.5

Figure 4.7: Unit cell of **compound 4.5** as determined by single crystal XRD. The compound crystallizes as 1-D polymeric trans-fashion zigzag chains. Void space between packing of 1-D polymeric chains is occupied by chlorobenzene guest molecules.

Although the space group and asymmetric unit are essentially the same as **compounds 2.1** and **4.4**, this structure differs in the connectivity of the one dimensional

polymeric chain, and thus in its crystal packing. In **compounds 2.1** and **4.4** the 1,2-dpe ligands are arranged in a "cis" fashion with respect to the boronate diester part, and generate a square zigzag chain as seen in **Figure 2.3a**. In compound 4.5, the 1,2-dpe ligands are arranged in a "trans" fashion about the boronate diester part thus generating a "saw-tooth" like zigzag chain as shown in **Figure 4.8**.

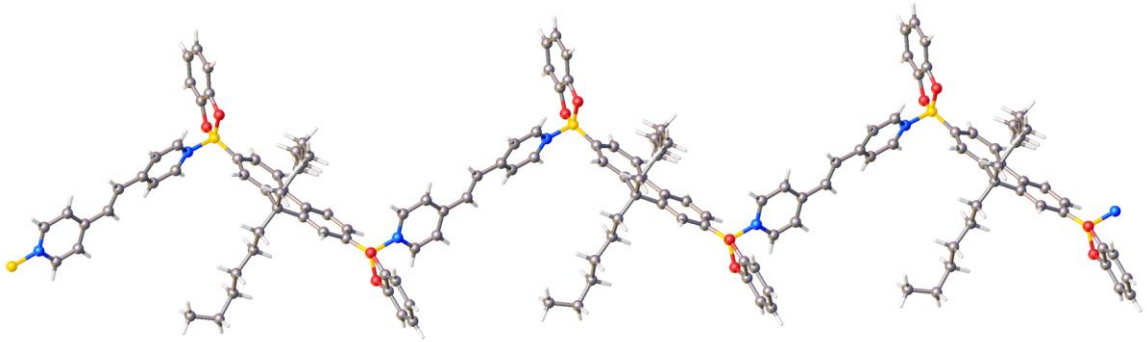

Figure 4.8: 1-D chain connectivity of **compound 4.5**. The 1,2-dpe ligands are arranged in a trans fashion about the boronate diester part generating a "saw-tooth" like zigzag chain as opposed to being arranged in a cis fashion about the boronate diester and generating a square zigzag chain as seen in **compound 2.1** and **4.4**.

Another notable difference in **compound 4.5** is that there are 2.5 chlorobenzene molecules per chain formula unit verses 2 benzene or fluorobenzene molecules in the "cis" fashion SMB coordination polymers. This gives **compound 4.5** a molecular formula of $[(C_{37}H_{40}B_2O_4)(C_{12}H_{10}N_2)]\cdot 2.5(C_6H_5Cl)$ which corresponds to 27.2% chlorobenzene by mass. It should be noted that the crystals grew in a very low yield and no further experiments were performed with this compound.

4.7 Bromobenzene SMB Coordination Polymer, Compound 4.6

Previous attempts to adsorb bromobenzene with desolvated **compound 2.1** proved inconclusive. I hypothesized that if bromobenzene was able to fit into the pores of **compound 2.1**, than recrystallization in bromobenzene would yield an identical SMB coordination polymer, but with different guest molecules as was observed in **compound**

4.4. A sample of desolvated **compound 2.1** was dissolved in hot bromobenzene, resulting in a transparent gold solution which was then allowed to cool slowly without disturbance. Slow evaporation over a two week period resulted in orange clusters of crystals of **compound 4.6**. The single crystal removed from a cluster of crystals was reported as a yellow rectangular plate crystal. Single crystal XRD analysis confirmed that **compound 4.6** crystallizes in the monoclinic space group $P2_1/n$ with the asymmetric unit consisting of one $[(C_{37}H_{40}B_2O_4)(C_{12}H_{10}N_2)]$ polymeric complex and three bromobenzene molecules as shown in **Figure 4.9**.

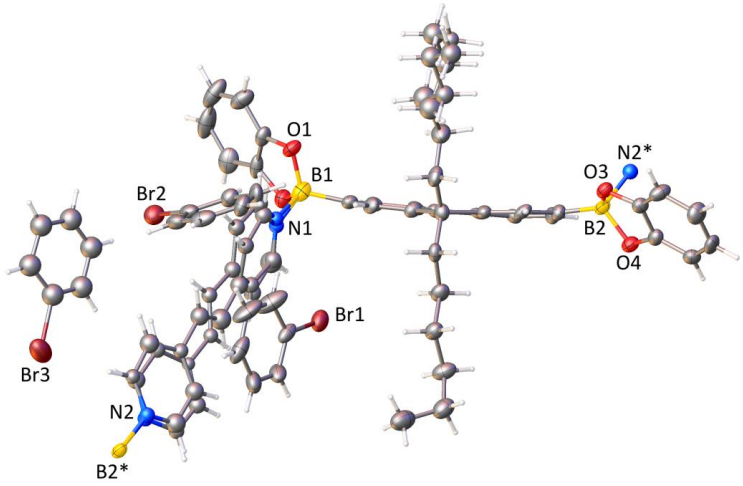

Compound 4.6

Figure 4.9: Unit cell of **compound 4.6** as determined by single crystal XRD. The compound crystallizes as 1-D polymeric trans-fashion zigzag chains identical to **compound 4.5**. Void space between packing of 1-D polymeric chains is occupied by bromobenzene guest molecules.

Structural solution reveals that **compound 4.6** is essentially identical to **compound 4.5**, but the guest molecules are bromobenzene in place of chlorobenzene. In **compound 4.6**, the 1,2-dpe ligands are arranged in a "trans" fashion about the boronate diester part, just like in **compound 4.5**, generating a "saw-tooth" like zigzag chain as

shown in **Figure 4.8**. Also, just like **compound 4.5**, there are 2.5 bromobenzene molecules per chain formula unit. This gives **compound 4.6** a molecular formula of $[(C_{37}H_{40}B_2O_4)(C_{12}H_{10}N_2)]\cdot 2.5(C_6H_5Br)$ which corresponds to 34.3% bromobenzene by mass. It should be noted that the crystallographer reported that these crystals were of low quality and the structure was difficult to refine. A TGA and ^1H NMR were collected for these crystals after they were isolated and dried under vacuum for 2.5 hours. The TGA revealed only a 14.3% mass loss due to bromobenzene which is significantly lower than the theoretical % mass of bromobenzene. This large difference may be due to the extended drying period under vacuum, or to the simple fact that upon exposure to air the crystals start to degrade and release their guest molecules.

4.8 Structural Analogues of Compound 2.1

Two analogues of **compound 2.1** were obtained by adding a methyl group at the 3 or 4 position of the catechol on the boronate diester portion and following the same synthetic scheme shown in **Figure 2.2**. It is anticipated that the electron donating methyl groups could induce red shifted optical transitions, as well as decrease pore size. XRD quality single crystals of the 4-methylcatechol analogue (**compound 4.7**) were obtained by recrystallization in dichloromethane, but quality single crystals of the 3-methylcatechol analogue have yet to be obtained. Refinement of the single crystal XRD data of **compound 4.7** reveals an asymmetric unit consisting of one $[(C_{39}H_{44}B_2O_4)(C_{12}H_{10}N_2)]$ polymeric repeating unit and two independent dichloromethane molecules. The crystal structure is very similar to **compound 2.1**, crystallizing in the same space group, $P2_1/n$ and exhibiting the same 1-D polymeric chain connectivity as shown in **Figure 4.10**.

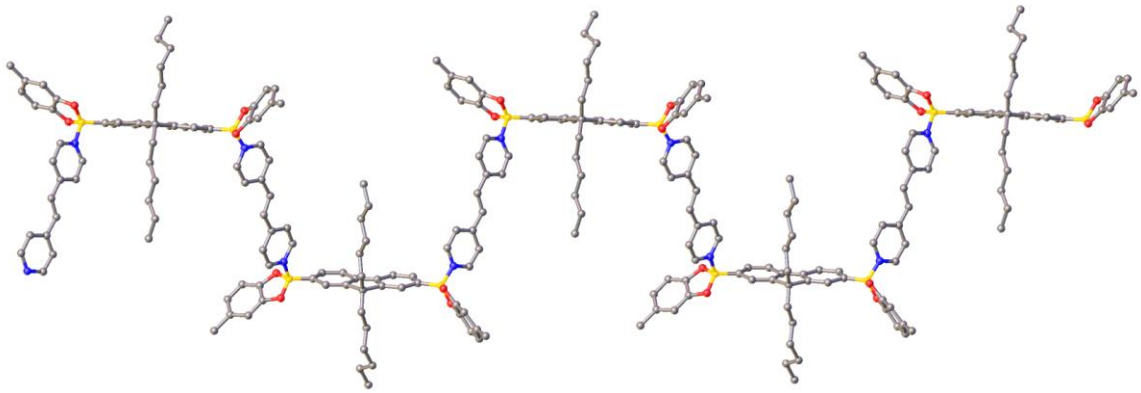

Compound 4.7

Figure 4.10: 1-D polymeric chain connectivity of **compound 4.7** which is identical to the chain connectivity of **compound 2.1**.

Even though the crystals of **compound 4.7** retain two CH_2Cl_2 molecules per unit, ^1H NMR and TGA on the initial powders of **compound 4.7** and the 3-methylcatechol analogue suggest that the compounds retain only small amounts of guest and do not maintain structural integrity upon guest removal.

The other analogue of **compound 2.1** was obtained by switching the diamine linker from 1,2-dpe to 4,4'-bipyridine (4,4'-bpy) while leaving the boronate diester backbone unchanged. Combining the boronate diester and 4,4'-bpy linker in a benzene reflux resulted in a transparent faint yellow solution. The solution was then allowed to cool slowly without disturbance which resulted in orange crystal clusters of **compound 4.8** overnight. The single crystal removed from a cluster of crystals was reported as a yellow plate crystal. Single crystal XRD analysis confirmed that **compound 4.8** crystallizes in the monoclinic space group $P2_1/n$ with the asymmetric unit consisting of one $[(C_{37}H_{40}B_2O_4)(C_{10}H_8N_2)]$ polymeric complex and two independent benzene molecules of crystallization as shown in **Figure 4.11a**.

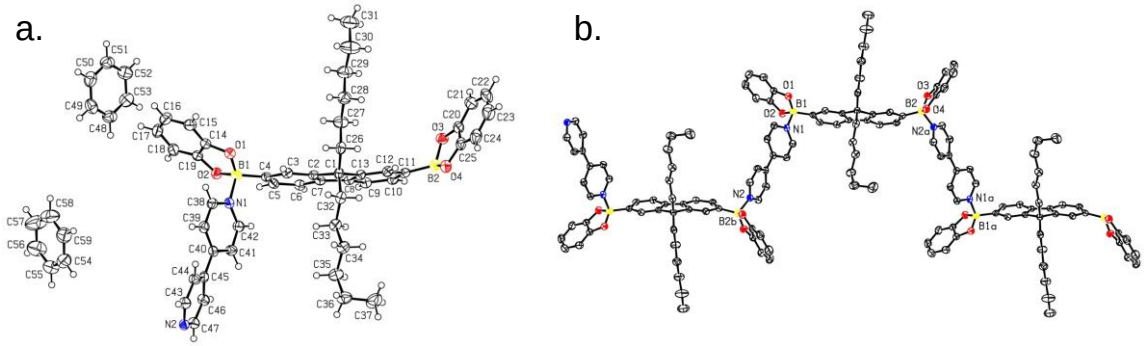

Figure 4.11: a. Unit cell of **compound 4.8** as determined by single crystal XRD. **b**. 1-D polymeric chain connectivity of **compound 4.8**. The chain connectivity is identical to that of **compound 2.1**

The 1-D polymeric chains have the same connectivity as **compound 2.1** which can be seen in **Figure 4.11b**. Also, a very similar feature is the inclusion of benzene between the packing of the polymeric chains. **Compound 4.8** hosts 2 benzene molecules per asymmetric unit, resulting in a molecular formula of $[(C_{37}H_{40}B_2O_4)(C_{10}H_8N_2)]\cdot 2C_6H_6$ which corresponds to a theoretical value of 17.7% benzene by mass. Experimental % mass benzene determined by TGA and ^{1}H NMR showed 18.2% and 17.2% respectively. It should be noted that a color change from orange to tan/brown was accompanied with the removal of benzene by TGA. When the tan/brown desolvated powder was soaked in liquid benzene overnight, the material re-adsorbed benzene and regained its orange color. This material may exhibit useful optical transitions associated with guest adsorption, but further studies are needed to understand the system.

4.9 Conclusion

In conclusion, we have discovered several new SMB networks by changing either the solvent of crystallization or the initial molecular building blocks. The discovery of these new networks further shows the solvent dependent structural polymorphism

associated with our system. It is interesting that changing the solvent alone can cause significant changes in the structural connectivity of the SMB network. Such structural changes suggest that the solvent interactions with the network play a large role in directing the connectivity of the network. Changing the initial building blocks used to form **compound 2.1** also yielded new SMB networks. We do not have enough preliminary results on these new structural analogues to determine their applicability for sensing or sequestration applications. There are still a lot of possible building blocks that we have yet to investigate to build new SMB networks. We have yet to alter the diboronic acid building block, as this may yield new SMB networks that exhibit interesting properties. Further investigation of the properties of our new SMB networks presented here is needed to determine their possible uses in applications, and there are many endless opportunities to synthesis new SMB networks using different building block that we have yet to investigate.

4.10 Experimental

Synthesis of xylenes inclusion macrocycle and hexagonal phase (compound 4.1): To a 250mL round bottom flask, 0.3018g (0.529mmol) boronate diester, 0.0971g (0.533mmol) 1,2-di-(4-pyridyl)ethylene, and 120mL xylenes (mixture of all isomers) were added. The solution was heated with stirring while open to air (no reflux condenser attached) for 5-10 minutes until all starting materials were dissolved. The faint yellow transparent solution was removed from heat and stirring and capped with a rubber septum before being put under a slow flow of nitrogen and allowed to cool undisturbed. Slow evaporation of the transparent yellow solution under a slow flow of nitrogen yielded yellow needle like crystals after 5 days. These crystals were found to be the hexagonal

phase structure. Our crystallographer reported that after submission of the sample, many large clusters of red crystals began appearing in the flask. After about 1 month all the yellow hexagonal phase crystals had converted to red macrocycle crystals. The solvent was decanted and the crystals were dried under vacuum for 1 hour before collection of red macrocycle crystals (0.4638g, 46.0% yield). ^{1}H NMR (300 MHz, CD_2Cl_2): δ 8.67-8.65 (q, 4H), 7.93 (s, 2H), 7.91-7.88 (d, 2H), 7.83-7.81 (d, 2H), 7.51-7.49 (q, 4H), 7.29 (s, 2H), 7.20-7.17 (q, 4H), 7.03-6.99 (q, 4H), 2.10-2.05 (m, 4H), 1.11-0.98 (m, 12H), 0.74-0.70 (t, 6H), 0.61-0.59 (m, 4H). All solvent peaks omitted.

Synthesis/crystallization of styrene inclusion macrocycle (compound 4.2): To a 205mL round bottom flask, 0.5104g (0.678mmol) of desolvated **compound 2.1** and 100mL of styrene were added. The solution was heated with stirring while open to air (no reflux condenser attached) for 5-10 minutes until all starting materials were dissolved. The transparent gold solution was removed from heat and stirring and capped with a rubber septum and 2 needles were put through the septum to allow for slow evaporation. After 5 days of slow evaporation a few red crystals appeared. The solution was then put under a slow flow of nitrogen and a day later the solution yielded a lot of red crystals. The solvent was decanted and the crystals were dried under vacuum for 45 minutes before collection of red macrocycle crystals (0.4644g, 71.3% yield). ^{1}H NMR (300 MHz, CD_2Cl_2): δ 8.68-8.66 (q, 4H), 7.93 (s, 2H), 7.90-7.88 (d, 2H), 7.83-7.81 (d, 2H), 7.51-7.49 (q, 4H), 7.29 (s, 2H), 7.20-7.17 (q, 4H), 7.02-6.99 (q, 4H), 2.10-2.05 (m, 4H), 1.02 (m, 12H), 0.74-0.70 (t, 6H), 0.56 (m, 4H). All solvent peaks omitted.

Synthesis of 3-methoxycatechol substituted boronate diester: To a 250mL round bottom flask, 0.4292g (1.017mmol) 9,9-dihexylfluorene-2,7-diboronic acid, 0.2849g

(2.033mmol) 3-methoxycatechol, and 150mL of toluene were added. A Dean Stark trap with 3Å molecular sieves activated by heating under vacuum for 5 minutes and a reflux condenser was attached to the reaction flask. The cloudy white solution was heated to reflux giving rise to a transparent solution. The solution was allowed to reflux overnight. After allowing the solution to cool the solvent was removed by rotary evaporation resulting in a white powder. The product, a white powder was dried under vacuum for 30 minutes before being collected (0.510g, 79.6% yield). ^{1}H NMR (300 MHz, CD_2Cl_2): δ 8.13 (s, 2H), 8.13-8.10 (d, 2H), 7.93-7.90 (d, 2H), 7.13-7.08 (t, 2H), 7.01-6.98 (d, 2H), 6.81-6.78 (d, 2H), 4.02 (s, 6H), 2.17-2.12 (m, 4H), 1.11-0.99 (m, 12H), 0.75-0.70 (t, 6H), 0.59 (m, 4H).

Synthesis of modified toluene inclusion macrocycle (compound 4.3): To a 100mL round bottom flask, 0.1216g (0.1929mmol) 3-methoxy substituted boronate diester, 0.0384g (0.1937mmol) 1,3-di-(4-pyridyl)propane, and 65mL of toluene. The transparent grey solution was attached to a reflux condenser and heated to reflux. Solution was allowed to reflux for 1 hour before cooling slowly without disturbance. No crystals grew upon cooling and the flask contained unwanted particulates. Solution was filtered via suction filtration before removing 30mL of solvent by rotary evaporation to make solution more concentrated. The concentrated solution was then heated with stirring while open to air (no reflux condenser attached) for 5-10 minutes. After removal from heat and stir the flask was capped with a rubber septum and the solution was put under a slow flow of nitrogen to enhance evaporation and crystal growth. After a few weeks clusters of yellow crystals grew and were analyzed by XRD. Unfortunately no yield or

further data on this sample was collected because the flask was dropped, broke and the entire product was lost.

Synthesis/crystallization of fluorobenzene inclusion SMB coordination polymer (compound 4.4): To a 250mL round bottom flask, 0.7734g (1.028mmol) of desolvated compound 2.1 and 150mL of fluorobenzene were added. The solution was heated with stirring while open to air (no reflux condenser attached) for 5-10 minutes until all starting materials were dissolved. The transparent gold solution was removed from heat and stirring and capped with a rubber septum and 2 needles were put through the septum to allow for slow evaporation. Small orange crystals grew overnight. The solvent was decanted and the crystals were dried under vacuum for 15 minutes before collection of the orange crystals (0.8217g, 84.6% yield). ^{1}H NMR (300 MHz, CD_2Cl_2): δ 8.68-8.66 (q, 4H), 7.92 (s, 2H), 7.89-7.86 (d, 2H), 7.82-7.80 (d, 2H), 7.52-7.49 (q, 4H), 7.29 (s, 2H), 7.19-7.16 (q, 4H), 7.01-6.98 (q, 4H), 2.10-2.04 (m, 4H), 1.08-1.01 (m, 12H), 0.74-0.70 (t, 6H), 0.59 (m, 4H). All solvent peaks omitted.

Synthesis/crystallization of chlorobenzene inclusion SMB coordination polymer (compound 4.5): To a 25mL round bottom flask, an unrecorded amount (<100mg) of desolvated compound 2.1 and 10mL chlorobenzene were added. The solution was heated with stirring while open to air (no reflux condenser attached) for 5-10 minutes until all starting materials were dissolved. The transparent yellow solution was allowed to undergo undisturbed slow evaporation upon which a few orange needle-like crystals grew after about 1 month. After single crystal XRD analysis the few crystals were re-dissolved in an attempt to recrystallize in a higher yield by using a slow flow of nitrogen. This attempt yield several orange crystals overnight. The solvent was decanted and the

crystals were dried under vacuum for 30 minutes. No yield could be calculated do to the unknown amount of starting material. ^{1}H NMR (400 MHz, CD_2Cl_2): δ 8.69-8.67 (q, 4H), 7.89 (s, 2H), 7.85-7.83 (d, 2H), 7.80-7.78 (d, 2H), 7.53-7.51 (q, 4H), 7.30 (s, 2H), 7.16-7.14 (q, 4H), 6.99-6.97 (q, 4H), 2.08-2.04 (m, 4H), 1.09-0.95 (m, 12H), 0.74-0.70 (t, 6H), 0.57-0.56(m, 4H). All solvent peaks omitted.

Synthesis/crystallization of bromobenzene inclusion SMB coordination polymer (compound 4.6): To a 25mL round bottom flask, an unrecorded amount (<100mg) of desolvated compound 2.1 and 15mL bromobenzene were added. The solution was heated with stirring while open to air (no reflux condenser attached) for 5-10 minutes until all starting materials were dissolved. The transparent gold solution was removed from heat and stirring and capped with a rubber septum and 2 needles were put through the septum to allow for slow evaporation. After 10 days, no crystals were present. A slow nitrogen flow was put over the solution to see if it would help crystal growth. The slow flow of nitrogen helped to yield orange crystals after 3 days. The crystals were collected by suction filtration and dried under vacuum for 2 hours and 20 minutes. No yield could be calculated do to the unknown amount of starting material. ^{1}H NMR (400 MHz, CD_2Cl_2): δ 8.70-8.68 (q, 4H), 7.87 (s, 2H), 7.82-7.80 (d, 2H), 7.79-7.77 (d, 2H), 7.54-7.52 (q, 4H), 7.30 (s, 2H), 7.14-7.12 (q, 4H), 6.97-6.94 (q, 4H), 2.07-2.03 (m, 4H), 1.09-0.96 (m, 12H), 0.74-0.70 (t, 6H), 0.59-0.55 (m, 4H). All solvent peaks omitted.

Synthesis of 3-methylcatechol substituted boronate diester: To a 250mL round bottom flask, 0.1466g (0.347mmol) 9,9-dihexylfluorene-2,7-diboronic acid, 0.0865g (0.697mmol) 3-methylcatechol, and 90mL benzene were added. A Dean Stark trap with 3Å molecular sieves activated by heating under vacuum for 5 minutes and a reflux

condenser was attached to the reaction flask. The solution was refluxed overnight with stirring, under a nitrogen atmosphere at 110°C. The resultant clear solution was allowed to cool to room temperature before being filtered by suction filtration to remove un-dissolved particulates. The transparent filtrate was transferred back to a round bottom flask before the benzene was removed by rotary evaporation leaving behind a white solid. The product, a white powder was dried under vacuum for 50 minutes (0.1600g, 77.1% yield). ^{1}H NMR (300 MHz, $CDCl_3$): δ 8.15-8.12 (d, 2H), 8.09 (s, 2H), 7.90-7.88 (d, 2H), 7.19-7.16 (d, 2H), 7.07-7.01 (t, 2H), 6.98-6.95 (d, 2H), 2.52 (s, 3H), 2.18-2.10 (m, 4H), 1.12-1.04 (m, 12H), 0.75-0.71 (t, 6H), 0.62 (m, 4H).

Synthesis of 4-methylcatechol substitued boronate diester: To a 205mL round bottom flask, 0.3170g (0.751mmol) 9,9-dihexylfluorene-2,7-diboronic acid, 0.1904g (1.53mmol) 4-methylcatechol, and 150mL benzene were added. A Dean Stark trap with 3Å molecular sieves activated by heating under vacuum for 5 minutes and a reflux condenser was attached to the reaction flask. The initial murky white solution gave rise to a transparent solution after 15 minutes of heating. The solution was refluxed overnight with stirring, under a nitrogen atmosphere at 110°C. The resultant clear solution was allowed to cool to room temperature before being filtered by suction filtration to remove un-dissolved particulates. The transparent filtrate was transferred back to a round bottom flask before the benzene was removed by rotary evaporation leaving behind a gray solid. The product, a gray powder was purified by vacuum sublimation for 6 hours at 120°C (0.3500g, 77.9% yield). ^{1}H NMR (300 MHz, $CDCl_3$): δ 8.12-8.09 (m, 4H), 7.90-7.88 (d, 2H), 7.23-7.21 (d, 2H), 7.17 (s, 2H), 6.96-6.93 (d, 2H), 2.44 (s, 3H), 2.14-2.10 (m, 4H), 1.04 (br m 12H), 0.76-0.72 (t, 6H), 0.63 (m, 4H).

Synthesis of SMB coordination polymer using 3-methylcatechol boronate diester: To a 250mL round bottom flask, 0.1500g (0.251mmol) 3-methylcatechol boronate diester, 0.0900g (0.494mmol) 1,2-di-(4-pyridyl)ethylene, and 85mL benzene were added. The solution was allowed to reflux for 30 minutes with stirring. The solution was then allowed to cool slowly without disturbance. Crystals did not grow upon cooling and slow evaporation. Benzene was removed by rotary evaporation leaving behind an oragne powder, (0.1284g, 65.5% yield). ^{1}H NMR (300 MHz, $CDCl_3$): δ 8.67-8.65 (q, 4H), 8.08-8.05 (d, 2H), 8.04 (s, 2H), 7.87-7.85 (d, 2H), 7.44-7.42 (q, 4H), 7.26 (s, 2H), 7.14-7.12 (d, 2H), 7.03-6.97 (t, 2H), 6.94-6.92 (d, 2H), 2.50 (s, 3H), 2.14-2.08 (m, 4H), 1.12-1.03 (m, 12H), 0.75-0.70 (t, 6H), 0.61 (m, 4H).

Synthesis of SMB coordination polymer using 4-methylcatechol boronate diester (compound 4.7): To a 250mL round bottome flask, 0.3296g (0.551mmol) 4-methylcatechol boronate diester, 0.1034g (0.567mmol) 1,2-di-(4-pyridyl)ethylene, and 105mL benzene were added. The solution was allowed to reflux for 30 minutes with stirring. The transparent yellow solution was then allowed to cool slowly without disturbance. Crystals did not grow upon cooling and slow evaporation. Benzene was removed by rotary evaporation leaving behind an orange crystalline powder, (0.4313g, 100% yield). Crystals for XRD were obtained by slow evaporation in dichloromethane, giving red crystals. ^{1}H NMR (300 MHz, CD_2Cl_2): δ 8.67-8.65 (q, 4H), 7.92 (s, 2H), 7.89-7.86 (d, 2H), 7.82-7.80 (d, 2H), 7.50-7.49 (q, 4H), 7.29 (s, 2H), 7.06-7.03 (d, 2H), 7.01 (s, 2H), 6.82-6.80 (d, 2H), 2.36 (s, 3H), 2.09-2.04 (m, 4H), 1.08-1.02 (m, 12H), 0.75-0.70 (t, 6H), 0.58 (m, 4H).

Synthesis of benzene inclusion SMB coordination polymer 4,4'-bipyridine analouge (compound 4.8): To a 250mL round bottom flask, 0.3970g (0.6961mmol) boronate diester, 0.1090g (0.6979mmol) 4,4'-bipyridine, and 100mL of benzene were added. The solution was allowed to reflux for 15 mintues under a nitrogen atmosphere giving rise to a transparent yellow solution with some undissolved particulates. A hot filtration was performed by suction filtration into a clean 250mL round bottom flask. The filtrate was heated to reflux before allowing to cool slowly without disturbance. Slow cooling did not result in crystals. Solution was then concentrated by removing about 40mL of benzene by rotary evaporation. The concentrated solution was reheated with stirring while open to air (no reflux condenser attached) for 5-10 minutes. The solution was then placed under a slow flow of nitrogen and allowed to cool slowly without disturbance. Cluster of orange crystals grew overnight. The solvent was decanted and the crystals were dried under vacuum for 15 minutes (0.3440g, 56.0% yield). ^{1}H NMR (400 MHz, CD_2Cl_2): δ 8.82-8.80 (q, 4H), 7.96 (s, 2H), 7.91-7.89 (d, 2H), 7.84-7.82 (d, 2H), 7.65-7.63 (q, 4H), 7.21-7.18 (q, 4H), 7.03-7.00 (q, 4H), 2.11-2.07 (m, 4H), 1.10-0.97 (m, 12H), 0.74-0.70 (t, 6H), 0.62-0.58 (m, 4H). Benzene solvent peak omitted.

General procedure for solvent soaks: To a 1 dram vial, 30-100mg of sample and 2mL of solvent are added. Vial is capped and allowed to sit for desired amount of time. The sample is recollected via suction filtration using a side arm flask and hirsh filter funnel. The recollected sample is transferred from filter paper to a clean vial and dried under vacuum for 15 minutes.

General procedure for vapor soaks: To a 10mL beaker, 30-150mg of sample are added. The beaker is then placed in a TLC chamber to which about 50mL of desired

solvent is added. The chamber is closed and allowed to sit undisturbed for desired amount of time. After the soak the beaker is removed from the chamber and the sample is transferred to a clean vial and dried under vacuum for 15 minutes.

Methods for determination of percent toluene: The methods for determination of percent of guests in the networks are the same as those for **compound 2.1** which are described in detail in the experimental section of **Chapter 2**.

4.11 References

[1] Nishiyabu, R.; Kubo, Y.; James, T. D.; Fossey, J. S. Boronic Acid Building Blocks: Tools for Self Assembly. *Chem. Commun.* **2011**, *47*, 1124-1150.

[2] Cote, A. P.; El-Kaderi, H. M.; Furukawa, H.; Hunt, J. R.; Yaghi, O. M. Reticular Synthesis of Microporous and Mesoporous 2D Covalent Organic Frameworks. *J. Am. Chem. Soc.* **2007**, *129*, 12914-12915.

[3] Hunt, J. R.; Doonan, C. J.; LeVangie, J. D.; Cote, A. P.; Yaghi, O. M. Reticular Synthesis of Covalent Organic Borosilicate Frameworks. *J. Am. Chem. Soc.* **2008**, *130*, 11872-11873.

[4] Yaghi, O. M.; O'Keeffe, M.; Ockwig, N. W.; Chae, H. K.; Eddaoudi, M.; Kim, J. Reticular Synthesis and the Design of New Materials. *Nature.* **2003**, *423*, 705-714.

[5] Christinat, N.; Croisier, E.; Scopelliti, R.; Cascella, M.; Rothlisberger, U.; Severin, K. *Eur. J. Inorg. Chem.* **2007,** 5177-5181.

[6] Jetti, R. K. R.; Kuduva, S. S.; Reddy, D. S.; Xue, F.; Mak, T. C. W.; Nangia, A.; Desiraju, G. R. 4-(Triphenylmethyl)benzoic Acid: a Supramolecular Wheel-and-Axle Host Compound. *Tetrahedron Letters.* **1998**, *39*, 913-916.

Bibliography

Biradha, K.; Hongo, Y.; Fujita, M. Crystal-to-Crystal Sliding of 2D Coordination Layers Triggered by Guest Exchange. *Angew. Chem. Int. Ed.* **2002**, *41*, 3395-3398.

Chadha, R.; Arora, P.; Saini, A.; Jain, D. S. Solvated Crystalline Forms of Nevirapine: Thermoanalytical and Spectroscopic Studies. *AAPS Pharm. Sci. Tech.* **2010**, *11*, 1328-1339.

Christinat, N.; Croisier, E.; Scopelliti, R.; Cascella, M.; Rothlisberger, U.; Severin, K. Formation of Boronate Ester Polymers with Efficient Intrastrand Charge-Transfer Transitions by Three-Component Reactions. *Eur. J. Inorg. Chem.* **2007**, 5177-5181.

Christinat, N.; Scopelliti, R.; Severin, K. Multicomponent Assembly of Boronic Acid Based Macrocycles and Cages. *Angew. Chem. Int. Ed.* **2008**, *47*, 1848-1852.

Cote, A. P.; Benin, A. I.; Ockwig, N. W.; O'Keeffe, M.; Matzger, A. J.; Yaghi, O. M. Porous, Crystalline, Covalent Organic Frameworks. *Science*, **2005**, *310*, 1166-1170.

Cote, A. P.; El-Kaderi, H. M.; Furukawa, H.; Hunt, J. R.; Yaghi, O. M. Reticular Synthesis of Microporous and Mesoporous 2D Covalent Organic Frameworks. *J. Am. Chem. Soc.* **2007**, *129*, 12914-12915.

Drew, S.; Smith, L.; McGee, K.; Mann, K. A Platinum(II) Extended Linear Chain Material That Selectively Uptakes Benzene. *Chem. Mater.* **2009,** *21*, 3117-3124.

Fujita, N.; Shinkai, S.; James, T. D. Boronic Acids in Molecular Self-Assembly. *Chem. Asian J.* **2008,** *3*, 1076-1091.

Goncalves, R. M. The Enthalpy and Entropy of Cavity Formation in Liquids and Corresponding States Principle. *Can. J. Chem.* **1990**, *68*, 1937-1949.

Hunt, J. R.; Doonan, C. J.; LeVangie, J. D.; Cote, A. P.; Yaghi, O. M. Reticular Synthesis of Covalent Organic Borosilicate Frameworks. *J. Am. Chem. Soc.* **2008**, *130*, 11872-11873.

Icli, B.; Sheepwash, E.; Riss-Johannessen, T.; Schenk, K.; Filinchuk, Y.; Scopelliti, R.; Severin, K. Dative Boron–Nitrogen Bonds in Structural Supramolecular Chemistry: Multicomponent Assembly of Prismatic Organic Cages. *Chem. Sci.* **2011,** *2*, 1719-1721.

Iwasawa, N.; Takahagi, H. Boronic Esters as a System for Crystallization-Induced Dynamic Self-Assembly Equipped with an "On−Off" Switch for Equilibration. *J. Am. Chem. Soc.* **2007,** *129,* 7754-7755.

Janiak, C. Engineering Coordination Polymers Towards Applications. *Dalton Trans,* **2003**, 2781-2804.

Janiak, C.; Vieth, J. K. MOFs, MILs and More: Concepts, Properties and Applications for Porous Coordination Networks (PCNs). *New J. Chem.* **2010**, *34*, 2366-2388.

Jetti, R. K. R.; Kuduva, S. S.; Reddy, D. S.; Xue, F.; Mak, T. C. W.; Nangia, A.; Desiraju, G. R. 4-(Triphenylmethyl)benzoic Acid: a Supramolecular Wheel-and-Axle Host Compound. *Tetrahedron Letters.* **1998**, *39*, 913-916.

Kitagawa, S.; Uemura, K. Dynamic Porous Properties of Coordination Polymers Inspired by Hydrogen Bonds. *Chem. Soc. Rev.* **2005**, *34*, 109-119.

Kitamura, M. Strategy for Control of Crystallization of Polymorphs. *Cryst. Eng. Comm.* **2009**, *11*, 949-964.

Larson, A. C.; Von Dreele, R. B. General Structure Analysis System (GSAS). *Los Alamos National Laboratory Report LAUR*. **1994**, 86-748.

Liu, J.; Lavigne, J. In *Boronic Acids: Preparation and Applications in Organic Synthesis, Medicine and Materials;* 2nd Ed. Hall, D., Ed.; Wiley-VCH: Weinheim, Germany, 2011; Vol. 2, pp 621-676.

Nishio, M. CH/π Hydrogen Bonds in Crystals. *Cryst. Eng. Comm.* **2004**, *6(27)*, 130-158.

Nishiyabu, R.; Kubo, Y.; James, T. D.; Fossey, J. S. Boronic Acid Building Blocks: Tools for Self Assembly. *Chem. Commun.* **2011**, *47*, 1124-1150.

Niu, W.; O'Sullivan, C.; Rambo, B. M. Smith, M. D.; Lavigne, J. J. Self-Repairing Polymers: Poly(dioxaborolane)s Containing Trigonal Planar Boron. *Chem. Commun*. **2005**, 4342-4344.

PEDCo Environmental. *International Benzene Regulations.* PEDCo Environmental Inc. Cincinnati, Ohio, 1977.

Peng, R.; Deng, S-R.; Li, M.; Li, D.; Li, Z-Y. Solvent-Dependent Copper(I) Conformational Supramolecular Pseudo-Polymorphs Based on a Flexible Thioether Ligand. *Cryst. Eng. Comm.* **2008**, *10*, 590-597.

Rambo, B. M.; Lavigne, J. J. Defining Self-Assembling Linear Oligo(dioxaborole)s. *Chem. Mater*. **2007**, *19*, 3732-3739.

Rambo, B. R.; Tilford R. W.; Lanni, L. M.; Liu, J.; Lavigne, J. J. Boronate-Linked Materials: Ranging from Amorphous Assemblies to Highly Structured Networks. In *Macromolecules Containing Metal and Metal-like Elements*, Abd-El-Aziz, A. S.; Carraher Jr., C. E.; Pittman Jr., C. U.; Zeldin, M. Ed. John Wiley & Sons, Inc.: Hoboken, New Jersey, 2009; Vol. 9, pp 255-294.

Reinhold, C. Metal-Organic Frameworks Take on New Structure: Porous Materials. *Mater. Today.* **2007**, *10*, 10.

Sapp, K. M.S. Dissertation, University of South Carolina, 2011.

Severin, K. Boronic Acids as Building Blocks for Molecular Nanostructures and Polymeric Materials. *Dalton Trans.* **2009**, 5254-5264.

Sheepwash, E.; Krampl, V.; Scopelliti, R.; Sereda, O.; Neels, A.; Severin, K. Molecular Networks Based on Dative Boron-Nitrogen Bonds. *Angew. Chem. Int. Ed*. **2011**, *50*, 3034-3037.

Sinnokrot, M. O.; Valeev, E. F.; Sherrill, C. D. Estimates of the Ab Initio Limit for π-π Interactions: The Benzene Dimer. *J. Am. Chem. Soc.* **2002**, *124*, 10887-10893.

Spek, A. L. Structure Validation in Chemical Crystallography. *Acta Cryst.* **2009**, *D65*, 148-155.

Tilford, R. W.; Gemmil, W. R.; zur Loye, H.-C.; Lavigne, J. J. Facile Synthesis of a Highly Crystalline, Covalently Linked Porous Boronate Network. *Chem. Mater*. **2006**, *18*, 5296-5301.

Tilford, R. W.; Mugavero, S. J.; Pellechia, P. J.; Lavigne, J. J. Tailoring Microporosity in Covalent Organic Frameworks (COFs). *Adv. Mater*. **2008**, *20*, 2741-2746.

Toby, B. H. EXPGUI, a Graphical User Interface for GSAS. *J. Appl. Cryst*. **2001**, *34*, 210-213.

Uemura, K.; Kitagawa, S.; Fukui, k.; Saito, K. A Contrivance for a Dynamic Porous Framework: Cooperative Guest Adsorption Based on Square Grids Connected by Amide-Amide Hydrogen Bonds. *J. Am. Chem. Soc.* **2004**, *126*, 3817-3828.

Uemura, K.; Matsuda, R.; Kitagawa, S. Flexible Microporous Coordination Polymers. *Journal of Solid State Chemistry.* **2005**, *178*, 2420-2429.

Veen, J.; Saini, D.; Hal, R.; Heimovaara, T. *Development of an optical sensor for BTEX and chlorinated ethylenes.* NOBIS-project:97-1-09.

Weijun, N.; Smith, M. D.; Lavigne, J. J. Self-Assembling Poly(dioxaborole)s as Blue-Emissive Materials. *J. Am. Chem. Soc*. **2006**, *128*, 16466-16467.

Yaghi, O. M.; O'Keeffe, M.; Ockwig, N. W.; Chae, H. K.; Eddaoudi, M.; Kim, J. Reticular Synthesis and the Design of New Materials. *Nature.* **2003**, *423*, 705-714.

Yu, L. Survival of the Fittest Polymorph: How Fast Nucleater Can Lose to Fast Grower. *Cryst. Eng. Comm.* **2007**, *9*, 847-851.